Combining reversible interactions and controlled degradation for hydrogel-only pulsatile protein release

By JIAWEI ZHANG, B. Sc.

A Thesis Submitted to the School of Graduate Studies in Partial Fulfillment of the Requirements for the Degree Master of Science

McMaster University MASTER OF SCIENCE (2022) Hamilton, Ontario (Chemistry)

TITLE: Combining reversible interactions and controlled degradation for hydrogel-only pulsatile protein release

AUTHOR: Jiawei Zhang, BSc. (McMaster University) SUPERVISOR: Dr. Ryan G. Wylie.

NUMBER of PAGES: x, 54

Acknowledgements

I would like to thank Dr. Ryan Wylie for his willingness to provide mentorship to advance my thesis project. Your insight and guidance are invaluable to my graduate career. To Dr. Vincent Huynh, for introducing me to the art of bioconjugation and controlled drug delivery. To April Marple and Mandeep Marway, for helping troubleshoot and optimising cell culture protocols. To Alex Jesmer, for your constructive feedback on my experiment design and data analysis processes. To Drs. Boyang Zhang and Paul Harrison, for providing HUVEC cells and silica gel, respectively. To Drs. Katherine Bujold and Jakob Magolan, for being part of my committee. To the NMR, Mass Spectrum, Biointerface Institute facilities, Bujold Lab, and Melacini Lab for usage of equipment.

Special thanks to my friends and family members for their continuous endorsement and encouragement throughout this journey. To Katherine Hartman for your great help and contributions on the fencing team. To Dr. Xiuping Ding, Dawn Lin, Yue Su, Feng Zhang, Anthony D'Angelo, Kevin Wai, Kevin Zhou, and members on the fencing team, for good company. And finally, to my parents, for your understanding and unconditional love during challenging times. I am beyond grateful to all of you and cannot appreciate your support enough.

Abstract:

Due to transport barriers and biological responses, repeated local injections are often required to achieve efficacy for protein-based therapeutics and vaccines. Strategies to achieve timed burst releases of proteins with a single injection are being developed to avoid the need for multiple injections, especially for high-risk injections or the treatment of remote populations. Herein, we report the first hydrogel platform that tunes two burst releases of a therapeutic antibody, bevacizumab, by combining an iminoboronate affinity release system with controlled hydrogel hydrolysis. The first burst release is controlled by the protein-iminoboronate reversible covalent interaction, where iminoboronate is immobilized to the polymer network, and can be tuned by (1) using a protein modified with oxyamine moieties to enhance complex formation, and (2) the inclusion of fructose, which decreases the strength of the protein-iminoboronate interaction. Protein release from hydrogels with affinity-controlled release mechanisms, which is similar to the reversible protein-iminoboronate interaction, often plateaus, which reserves protein for the second burst release. The timing of the second burst release, which comprises of terminating protein after the initial burst, is then controlled by the hydrolytic crosslink, which occurred ~3-4 weeks after initial hydrogel formation. Hydrogel degradation rates can be further tuned by altering hydrolysis kinetics. Therefore, affinity release in combination with controlled degradation allows for the construction of hydrogel platforms to achieve two burst releases from a single injection.

List of Figures

List of tables

List of abbreviations

- ^{1}H NMR: proton nuclear magnetic resonance
- 2-APBA: 2-acetylphenylboronic acid
- ACVA: 4,4-azobis(4-cyanovaleric acid)
- AF-488: AlexFluor 488
- APMA: aminopropyl methacrylamide
- Az: azide
- BBB: blood-brain barrier
- BRB: blood-retinal barrier
- BSA: bovine serum albumin
- Bv: bevacizumab
- CB: carboxybetaine
- CPAD: 4-cyano-4-(phenylcarbonothioylthio)pentanoic acid
- CRA: cytokine release assay
- DBCO: dibenzocyclooctyne
- DMSO: dimethyl sulfonate
- DMSO: dimethyl sulfoxide
- DOL: degree of labelling
- EDC: 1-Ethyl-3-(3-dimethylaminopropyl)carbodiimide
- EGM-2: endothelial cell growth media 2
- ELISA: enzyme-linked immunosorbent assay
- ESI-TOF MS: electrospray ionization-time of flight mass spectrometry
- FBS: fetal bovine serum
- GPC: gel permeation chromatography
- HPLC: high pressure liquid chromatography
- HUVEC: Human umbilical vein endothelial cells
- IFN-γ: interferon gamma
- IL-6: interleukin 6
- kDA: kilodalton
- LPS: lipopolysaccharide
- MALDI-TOF MS: matrix-assisted laser desorption/ionization-time of flight mass spectrometry
- M_n: number average molecular weight
- MW: molecular weight
- M_w: weight average molecular weight
- NHS-AZ: succinimidyl carbonate azides
- NHS-DBCO: succinimidyl carbonate dibenzocyclooctyne
- NHS: N-hydroxysuccinimide
- Oxy-Bv: oxyaminated bevacizumab
- Oxyamine/oxy: O, O'-1, 3-Propanediylbishydroxylamine
- PBS: Phosphate buffered saline
- pCB: poly(carboxybetaine)
- PLGA: poly(lactide-co-glycolide)
- RAFT: reversible addition-fragmentation chain-transfer

- rhVEGF: recombinant human vascular endothelial growth factor
- SEC: size exclusion chromatography
- SPAAC: strain-promoted alkyne-azide cycloaddition
- TNF-α: tumor necrosis factor alpha

Table of Contents

1 Introduction

1.1 Rational for the development of local protein delivery vehicles

Protein therapeutics have shown great promise in the treatment of brain tumors and ocular diseases, but local delivery strategies are required to achieve efficacy due to transport barriers, such as the blood brain barrier and blood retinal barrier [1,2]. As examples, *Gliadel* wafers that release chemotherapeutics are routinely implanted into brain tumor resection cavities to achieve therapeutic concentrations, and the administration of anti-VEGF antibodies for the treatment of retinal diseases requires intravitreal injections. Because invasive surgeries and injections are risky and may result in serious side effects, local delivery devices are required to minimize the number of interventions.

Protein based vaccines often required two or more doses to achieve long term efficacy [3,4]. Although multiple doses can be administered with multiple injections, there is a need to minimize injection numbers for remote communities with minimal health care access, where it has proven difficult to reach the same individual multiple times. Additionally, sustained release of each dose over a few days has been shown to further improve immunity[5]. Therefore, local delivery vehicles that can include multiple doses with release over a few days may prove useful for protein-based vaccines.

1.2 Goal, Hypothesis, and Objectives

Goal: To mimic multiple protein injections with a single administration, we will combine affinity-like release system with controlled hydrogel degradation to achieve a tunable and pulsatile release system for the local delivery of proteins from hydrogels. The work will help build towards protein delivery vehicles for sites with transport barriers that prevent intravenous administration (e.g. brain tumours and retinal tissue) and for vaccines that require multiple injections.

Hypothesis: The combination of an affinity-like protein release mechanism with controlled hydrolytic degradation within an injectable hydrogel will allow for tunable and biphasic pulsed release of a protein therapeutic.

Objectives:

1. **Affinity release through reversible covalent interactions within a hydrogel**. Injectable low-fouling poly(carboxybetaine) (pCB) hydrogels modified with iminoboronate for the formation of reversible interactions with amine groups on the encapsulated therapeutic protein were synthesized. Release profiles were characterized as a function of bevacizumab, an anti-VEGF therapeutic protein, concentrations.
2. **Demonstrating tunable release through protein modification and competitive ligands**. Release profiles of bevacizumab were then tuned by the modification of bevacizumab with oxyamines, to decrease the rate of release, and/or the inclusion of fructose to increase the rate of release.
3. **Demonstrating biphasic pulsatile release by combining affinity-like release with controlled hydrogel degradation**. By incorporating the affinity-like release system with a degradable pCB hydrogel, we achieved a tunable pulsatile release where bevacizumab was released as two bursts roughly 3 weeks apart.

4. **Characterisation of biocompatibility and bioactivity**. The bioactivity of oxyamine modified bevacizumab was confirmed by a HUVEC proliferation assay and the compatibility of the local delivery vehicles was assessed by a cytokine release assay in whole blood.

1.3 Pulsatile release systems

A single-injection, pulsatile release system provides ideal solution to mimic periodic injection regimens required by regular insulin intake, immunotherapy, or vaccination practices. Various polymeric systems have been explored to achieve pulsatile release profiles, which are often controlled by external or endogenous stimuli. For example, a thermo-responsive PIPAAm-grafted hydrogel was used to achieve temperature-controlled oscillating delivery[6]. In addition, a glucose-responsive insulin delivery system was developed using poly(PIPAAm-acrylamidephenylboronic acid) copolymer that degraded in the presence of glucose[7]. More stimuli-induced pulsatile release systems include electricity-controlled p(AMPS-co-BMA)[8], magnetic field-controlled ethylene vinyl acetate copolymer[9], or pH/cationic interactions-controlled with alginate[10]. These systems have demonstrated multi-phasic pulsed release of therapeutics within a period between several hours and up to two months. However, the necessity for specific stimuli limits their application for wide clinical practices.

First reported by Dr. Robert Langer [11], the poly(lactide-co-glycolide), or PLGA, microparticle-based drug release system has demonstrated a wide spectrum of release kinetics following apparent zero order[12], first order[12,13], second order[14], and pulsatile release[15–17]. Notably, multi-phasic pulsatile release from PLGA microparticles has been studied for a variety of therapeutics and vaccine antigens, ranging from small molecule drug[15,18], protein-based vaccine antigen[16], to novel dinucleotide-based cGAMP-STING antagonists[19]. As the release rate of

proteins from PLGA microparticles is determined via both drug diffusion rate and matrix-degradation kinetics, these microparticle systems are self-contained without the necessity for stimuli, and release profiles can be designed to suit specific needs. However, despite its advantages, tunability of PLGA-based release systems relies on increasingly elaborate structural designs, such as core/shell microparticles, thus requiring complex polymer formulation and manufacturing processes [20,21].

1.4 Injectable hydrogels in drug delivery

Hydrogels offer a simple platform for the local delivery of proteins, where protein therapeutics can simply be mixed with the polymer solution prior to injection. Hydrogels are materials formed by hydrophilic polymers undergoing three-dimensional (3-D) physical or chemical crosslinking in an aqueous environment, thus capable of retaining large amounts of water within its porous structure[22]. Consequently, high water content provides a suitable environment to encapsulated cells or drugs, particularly protein-based therapeutic[23].

[23]Hydrogels have been long established for delivery of hydrophilic, small molecule drugs and proteins. Due to their porous nature, most drug-loaded hydrogels would be depleted within only a few hours to at most a few days[23]. Thus, various mechanisms have been explored to exert control on therapeutic release profile, ranging from modifications on hydrogel microstructure to purpose-designed drug-hydrogel interactions[23]. Control over drug diffusion rate has been achieved via interpenetrating polymer networks[24], surface diffusion control[25] and introduction of secondary delivery vehicles[26]. Alternatively, moieties that allow ionic interactions with charged drugs can be incorporated into hydrogel structure, thus increasing drug-gel interactions to extend sustained release[27,28]. Furthermore, covalent conjugation is also commonly used to control release rates

where drug-polymer bonds include chemical or enzymatic cleavage sites, thus allowing the therapeutic to slowly hydrolyse and be released[29].

Injectable hydrogels have become a common material for drug delivery for the ease of drug loading, adaptable morphology, and minimal invasive processes for subsequent administration[30,31]. Specifically, therapeutics can be easily mixed in low-viscosity polymeric solution right before the hydrogel forms at diseased sites *in situ*. To achieve *in situ* gelation, several crosslinking mechanisms established as summarised in **Table 1-1**. One potential drawback of *in situ* gelation lies in the risk of syringe clogging, preventing subsequent injection. Nonetheless, this issue can be readily solved by tuning gelation time and viscosity during hydrogel design, granting sufficient time for preparation and eliminating the necessity for special equipment.

Table 1-1. Common *in situ* gelation stimuli or mechanism for injectable hydrogels.

Gelation stimuli or mechanism	Examples
Thermo-stimuli	Poloxamer[32]
pH-stimuli	Carbopol and Chitosan[33]
Ion-activated	Gellan Gum[34]
Click Chemistry	DBCO-HA & 4-arm PEG azide[35]

1.5 Affinity-based drug release systems from hydrogels for controlled protein delivery

Over the past 20 years, affinity mechanisms have been explored for protein delivery. Affinity-based drug release systems achieve control over drug release rate through reversible interactions between therapeutics and polymer matrix, where drug efflux rate would be attenuated via constant reversible association-dissociation reactions[36,37]. Among various affinity interactions Van der Waals force, hydrogen bonding, ionic interactions, and hydrophobic interactions

(commonly through known biological interactions) are most exploited mechanisms for this purpose[36].

Inspirations of affinity-based release systems first came from natural biological interactions, notably heparin and heparin-binding proteins[37]. Early attempts for protein delivery were made to deliver fibroblast growth factors, a protein useful for stimulating cell growth and tissue repairs but suffers from rapid degradation in conventional hydrogel matrix[38]. For example, functionalised heparin on alginate polymer allows stabilisation of fibroblast growth factor for prolonged storage and handling, with 87.5% of released in bioactive form[38].

Aside from heparin and heparin-mimic systems, other affinity systems explored for protein or peptide-based therapeutics include peptide-metal[39,40], protein-protein and DNA aptamer-protein interactions. Reversible covalent bonds have also been investigated for peptide delivery[41]. A synthetic cell-adhesive peptide model therapeutic was conjugated to a PEG hydrogel via thiol-maleimide Diels-Alder reaction, while the release profile was controlled by temperature. In this thesis, we explored the use of reversible small molecule interaction to eliminate the need for biological binding ligands that may result in unwanted biological responses, such as immune reactions to avidin, which has been used for affinity release.

Affinity release profiles are typically governed by the rate and equilibrium constants between protein therapeutics and the hydrogel. For most release profiles, the equilibrium constant will determine the amount of drug released in the initial burst followed by very slow or no release [37]. To increase release rate, displacement affinity release systems have been developed where the replenishment of a competitor ligand from sparingly soluble hydrogel encapsulated pellets allows for tunable release after the initial burst release[42,43]. Although for pulsatile release, affinity systems can be used to tune the initial burst release without the need for continual release. A second

mechanism, such as hydrogel degradation, can then be used to create the second burst release and achieve pulsatile release, as demonstrated in this thesis.

1.6 Zwitterionic and low-fouling hydrogels for local therapies

Biomaterials developed for clinical implantation should have minimal unwanted immune responses. One method to minimise unwanted immune responses is to minimise interactions with biological molecules and host cells. Zwitterionic polymers have demonstrated resistance against protein attachment through strong hydration, where formation of a water layer prevents protein from reaching polymeric surface[46]. In addition, zwitterionic hydrogels have also been shown to be minimise nonspecific cell attachment.

While structurally diverse, zwitterionic polymers can be identified by having both cationic and anionic groups with overall charge neutrality. Compared to poly-hydrophilic materials, zwitterionic moieties were shown to exhibit lower hydration free energy, allowing water molecules to bond in greater quantities because of electrostatic hydration[47]. An established zwitterionic polycarboxybetaine (pCB) hydrogel is well suited for drug delivery application. Poly(carboxybetaine-co-aminopropyl methacrylamide), or pCB-APMA copolymer, is low-fouling and non-immunogenic with little nonspecific protein or cell adsorption, while reactive amine sites on aminopropyl methacrylamide (APMA) side chains are readily available for modifications[48–50]. Previous studies have demonstrated that pCB hydrogel reduces 90% nonspecific cell adhesion compared to a non-zwitterionic hydrogel poly(2-hydroxyethyl methacrylate, a leading biomaterial, and low adsorption against proteins in various media, including plasma[51–53]. To summarise, a combination of anti-fouling properties and functionalisable sites makes pCB-APMA suitable for the construction of local protein delivery vehicles.

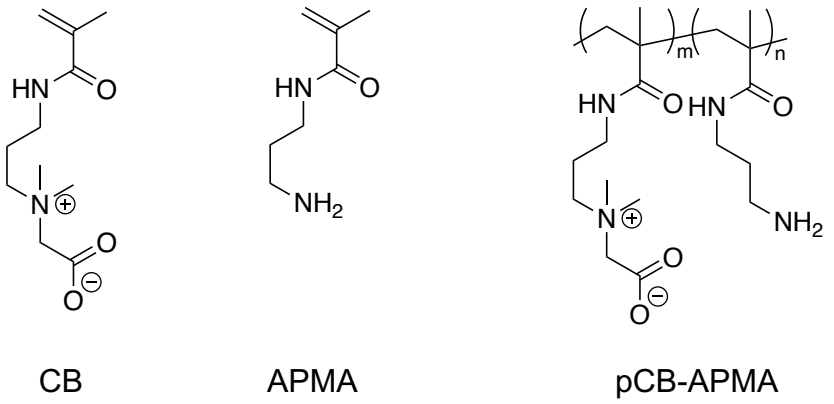

Figure 1-1. Zwitterionic structure of poly(carboxybetaine-co-aminopropyl methacrylamide), or pCB-APMA and its monomers.

1.7 Polymer synthesis via reversible-addition fragmentation chain-transfer (RAFT) reaction

Uniform chain length among pCB-APMA copolymer is required to ensure consistency in hydrogel formation. The RAFT reaction provides metal-free controlled radical polymerisation with predefined molecular weight, uniform dispersity at a range of temperature and reaction medium, including aqueous buffers[54,55]. In contrast to common free radical reactions, control over molecular weight and dispersity is achieved through degenerative transfer by chain transfer agents (CTA) in the form of thiocarbonylthiol compounds[56] (**Figure 1-2**). Specifically, radical species generated from the initiator are added to the CTA and subsequent equilibrium is reached between active and dormant chains, sometimes referred to as a macroCTA[56]. Due to higher rate of reversible addition/fragmentation equilibrium compared to chain propagation, per each cycle fresh monomers are added to only a portion of existing active chains, thus allowing a consistent degree of polymerisation and dispersity among all chains[56].

Figure 1-2. Generic structures of common chain transfer agents [57].

1.8 Strain-promoted alkyne-azide cycloaddition (SPAAC) affords *in situ* gelation

Among existing crosslinking options for injectable hydrogel (**Table 1-1**), a fast, non-toxic, biorthogonal, and biocompatible covalent crosslinking under physiological conditions is often preferred to achieve stable, irreversible bonding[22,58]. A selective and biorthogonal azide-alkyne cycloaddition "click" chemistry is well suited for this purpose without the need for external stimuli. Previous studies proposed ring strain as alternative mechanism to activate for azide [3+2] cycloaddition now known as SPAAC reaction[59]. This reaction allows "click" chemistry to occur under physiological conditions, a well-suited property for fast *in situ* gelation without introducing toxic catalyst. Specifically, APMA side chains on polymer backbone can be functionalised with azide and dibenzocyclooctyne (DBCO) groups, enabling *in situ* gelation via strain-promoted alkyne-azide cycloaddition (SPAAC) reaction (**Figure 1-3**)[60]. Azide-alkyne cycloaddition was originally developed in 1963 by Dr. Huisgen and improved by Sharpless et al with presence of copper (I) catalysis at physiological temperature[61]. However, copper-based catalysis is toxic and thus unfeasible for pharmaceutical applications in a clinical setting.

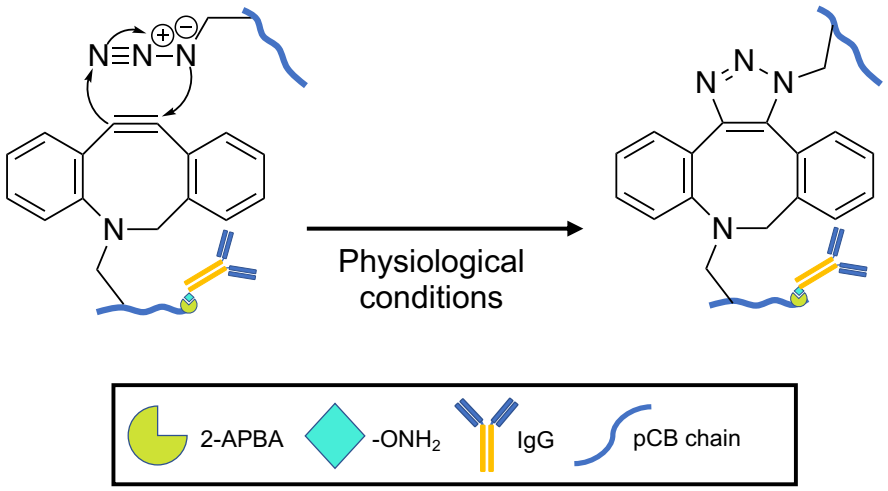

Figure 1-3. Schematic of strain-promoted alkyne-azide cycloaddition (SPAAC) reaction in hydrogel formation. Top pCB chain: pCB-azide polymer. Bottom pCB chain: pCB-(2-APBA)-DBCO with an antibody conjugated.

1.9 Pulsatile release through a hydrogel-only system

To achieve tunable and pulsatile release of proteins from a hydrogel without the need for external or endogenous stimuli, we combined the iminoboronate affinity system with controlled hydrolytic degradation of pCB hydrogels to develop a hydrogel-only pulsatile release system as described in Chapter 2. The development of hydrogel-only systems for pulsatile release can simplify the production of pulsatile delivery systems or expand the capabilities of PLGA systems using composite hydrogels to incorporate additional release pulses.

Iminoboronate can be formed by reacting 2-formyl phenylboronic acid (2-FPBA) or 2-acetyl phenylboronic acid (2-APBA) with a variety of nucleophilic groups under physiological conditions[64]. Its specific structure allows formed imine group to be activated by boronic acid and are kinetically prone to hydrolysis, thus providing stability of products and reversibility of conjugation [64,65]. Therefore, this reversible conjugation offers potential opportunity for controlling release rates of therapeutics from hydrogels.

Equation 1. $K_D = K_{off}/K_{on} = (C_{binding\ partner} \bullet C_{therapeutic})/C_{complex}$

Bond stability is a property reflected on the equilibrium dissociation constant and is known to play an important role in tailoring release profile in affinity-based drug delivery systems (**Equation 1**)[37]. Due to varying nucleophilicity, iminoboronate species formed between amine, oxyamine, or hydrazine moieties and 2-acetyl phenylboronic acids have exhibited dissociation constants (K_D) ranging from 10^{-3} to 10^{-8} M, allowing for a large range of release profiles suitable for varying therapeutics [65,66]. Moreover, previous studies have shown that iminoboronate dissociation can be further facilitated by several endogenous molecules, such as glutathione, dopamine, and fructose, which allows rapid release of over 50% conjugated butylamine within 100 minutes[63]. Consequently, dissociation of iminoboronate bond caused by the presence of biocompatible small molecules provides potential opportunities to tailor release rates, while simultaneously minimising the risk of adverse biological events.

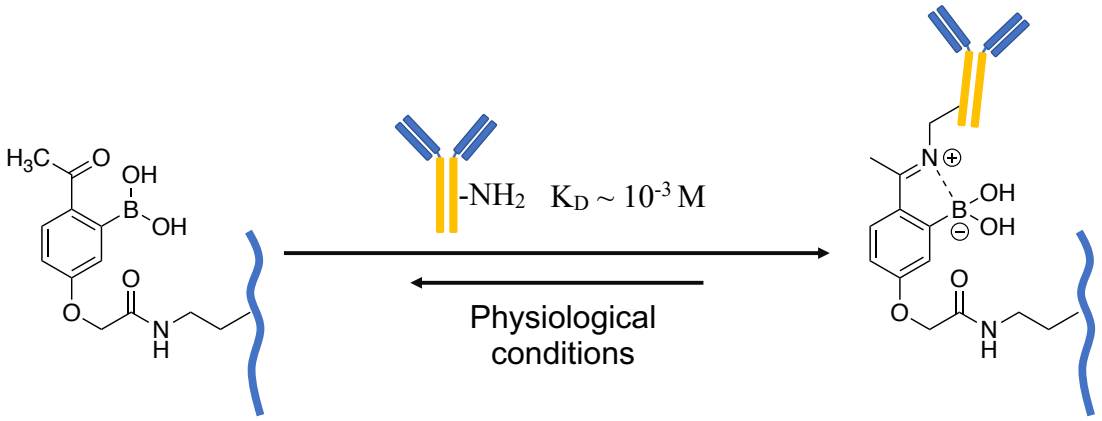

Figure 1-4. Schematic for iminoboronate formation and dissociation with surface amine groups on an antibody.

Hydrogel degradation is a necessary property in local drug delivery applications. Implanted or injected hydrogel must be degraded into non-toxic and non-immunogenic products that can subsequently be excreted from the diseased site. Common hydrogel degradation mechanisms include disulfide bond reduction, enzymatic digestion, and hydrolysis. Hydrolytic degradation can

remain consistent across physiological conditions, and thus provide a good control mechanism for our generalist approach towards pulsatile protein release. A previous reported degradable crosslinker, NHS-azide (Cl), was chosen for this project because of its predictable and tunable hydrolysis kinetics [67].

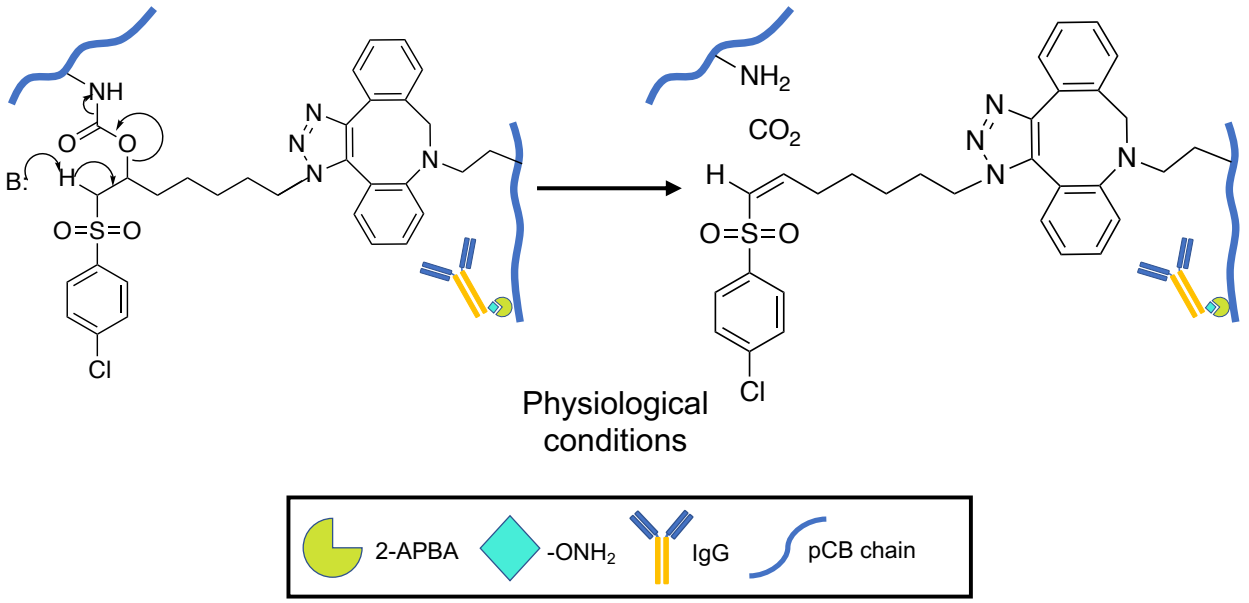

Figure 1-5. Hydrolysis mechanism of degradable crosslinker NHS-azide (Cl). Left: degradable pCB-azide (Cl) polymer with its degradable NHS-azide (Cl) crosslinker. Right: pCB-(2-APBA)-DBCO with an antibody conjugated.

2 Combining reversible interactions and controlled degradation for hydrogel-only pulsatile protein release

Jiawei Zhang and Ryan G. Wylie.

2.1 Introduction

The development of local delivery vehicles for protein therapeutics continues to be an active area of research to overcome transport barriers, to achieve dosing regimens with greater efficacy, and improve patient compliance and comfort. Protein therapeutics for diseases sites within the brain and the posterior segment of the eye are hindered by blood-tissue barriers, which often prevents the attainment of minimum effective concentrations after intravenous administration[69–72]. For example, antibodies or Fab fragments that neutralise vascular endothelial growth factor 165 (VEGF) to reduce angiogenesis in patients with retinal degenerative diseases, such as wet age-related macular degeneration and retinitis pigmentosa, are intravitreally injected every few weeks, which can lead to injection related tissue damage. High frequency dosing over a long period often results in inconsistent patient adherence rate, as low as 52%[73]. Therefore, injectable local delivery vehicles are being developed to minimise the number of injections.

Delivery vehicles can be designed to sustain release over several days to weeks or designed to achieve pulsatile release, where release occurs as bursts over a short time (e.g., hours to a few days) followed by no release until the next burst. Whereas sustained release systems aim to maintain stable concentrations, pulsatile release systems are designed to mimic repeated administrations with a single injection, and thus provide an effective solution to a variety of clinical practices ranging from reducing vaccine to insulin administrations. Meanwhile, effective vaccination often requires two or more injections separated by several weeks, yet strict storage conditions and transport logistics prove challenging for countries lacking in infrastructure and

healthcare resources to reach the same individual multiple times [74–76]. As a result, vaccine drop off rate is significantly higher in developing countries[77]. Pulsatile systems can also mimic the clinically established injection cycles of many protein therapeutics, such anti-VEGF treatments for retinal degenerative diseases. Therefore, their continues to remain a great need for pulsatile protein release, which has led to the development of stimuli-responsive and controlled degradation mechanisms.

End-user controlled stimuli-responsive drug release mechanisms have been developed using endogenous or external stimuli (e.g. temperature, glucose level, electricity, magnetic fields) after implantation of the delivery vehicle. Existing materials include a thermo-responsive PIPAAm-grafted hydrogel for temperature-controlled oscillating delivery[6], a glucose-responsive insulin delivery system using poly(PIPAAm-acrylamidephenylboronic acid) copolymer[7], as well as electricity-controlled p(AMPS-co-BMA)[8], and magnetic field-controlled ethylene vinyl acetate copolymer[9].

To avoid the need for stimuli, researchers have focused on the controlled degradation of biomaterials to achieve predetermined pulsatile release profiles. For example[11], the poly(lactide-co-glycolide) (PLGA) microparticle-based drug release system can be tuned for release kinetics that follow apparent zero order[12], first order[12,13], second order[14], and pulsatile release[15–17]. Notably, multi-phasic pulsatile release from PLGA microparticles has been studied on a variety of therapeutics and vaccine antigens, ranging from small molecule drug[15,18], protein-based vaccine antigen[16], to novel dinucleotide-based cGAMP-STING antagonists[19]. As the release rate of proteins from PLGA microparticles is determined via both drug diffusion rate and matrix-degradation kinetics, release profiles can be tailored for specific needs. A mixture of PLGA particles can therefore be used to achieve pulsatile release. Recently, pulsatile release of TGFβ

regulators was achieve by fabricating a composite hydrogel with PLGA particles, where the initial release occurred from drug dissolved within the hydrogel matrix and subsequent burst release from drug encapsulated within the PLGA particles[78]. The use of hydrogels may also prove beneficial by improving PLGA particle retention at the injection site. The use of PLGA systems therefore allows for the pulsatile release of protein therapeutics without the need for external stimuli.

To expand the pulsatile drug release potential of hydrogels, we took advantage of affinity-like drug release and controlled hydrogel degradation to achieve a tunable two-pulse release mechanisms without PLGA microparticles or the need for external stimuli. Hydrogel-only vehicles have the potential to simplify vehicle production and protein encapsulation procedures. Moreover, hydrogels with pulsatile release properties can be combined with PLGA particles to increase the number of pulsed releases. Affinity release systems, where the protein therapeutic reversibly interacts with the hydrogel polymer network, often result in a tunable burst release of proteins over the first few hours or days without complete release. The first burst release can therefore be tuned by altering the affinity of the polymer-protein interactions, with stronger interactions resulting in less release. By also incorporating controlled degradation, a second burst release can then be timed by the degradation rate of hydrogel polymers or crosslinks and the amount of protein released by tuning the size of the affinity controlled burst release. Hydrogel-only pulsatile release system may therefore expand and simplify pulsatile protein delivery without the need for external stimuli.

To establish a hydrogel-only pulsatile release systems, we developed a new affinity-like release system based on the reversible formation of iminoboronates within poly(carboxybetaine) (pCB) hydrogels crosslinked with electronically tunable and hydrolytic carbamate bonds. [62]A low-fouling polymer, pCB, was chosen for hydrogel formation to limit nonspecific protein-hydrogel interactions and allow for tunable protein release. For the grafting of 2-acetyl phenylboronic acid

(2-APBA) and azide or DBCO crosslinker moieties, we first synthesized a copolymer of p(carboxybetaine-co-aminopropyl methacrylamide) that contains primary amines. Upon hydrogel formation through SPAAC in the presence of antibody, the first burst release profile will be determined by the interaction of antibody amines with 2-APBA to form iminoboronates. Release rates can be further tuned by increasing the stability of the bond by the modification of the antibody with oxyamines or decreasing complexation by the inclusion of fructose, which is known to disrupt iminoboronate formation. The second burst release then occurs due to crosslink hydrolysis, which resulted in protein release after three weeks. Bevacizumab (Bv), also known as Avastin, is an FDA-approved human monoclonal IgG utilized for retinal degenerative diseases and certain cancers, and was chosen as a model protein to demonstrate pulsatile release[68]. Affinity-like release with controlled hydrogel degradation therefore allows for the formation of hydrogel-only pulsatile delivery vehicles for proteins.

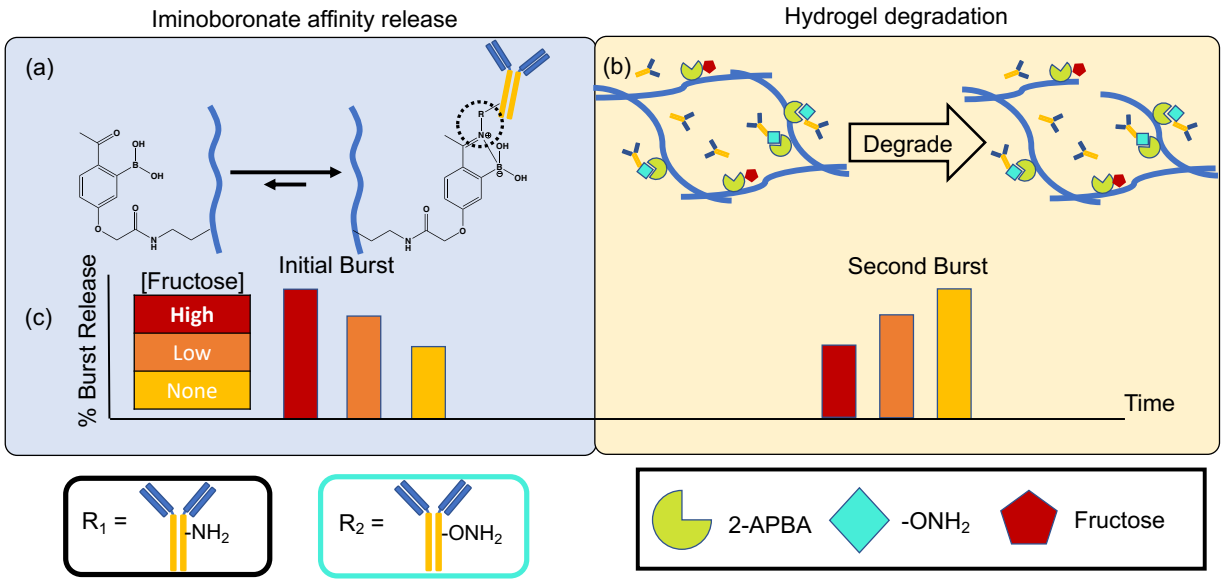

Figure 2-1. Schematics of injectable pCB-APBA hydrogels for controlled release of proteins. **(a)** Reversible iminoboronate bonds are formed between 2-APBA and nucleophilic groups, including amines and oxyamines, and dictate the size of the first burst release, which can be further tuned by

the inclusion of fructose. **(b)** Hydrogel degradation results in the second burst release to achieve biphasic pulsatile release.

2.2 Results and Discussion

2.2.1 Polymer synthesis and gelation time

The pCB-APMA random copolymer was synthesised by RAFT polymerisation (**Figure 2-2**) to achieve a suitable molecular weight (MW) and composition while maintain gelation potential and low-fouling properties, which was previously defined to be limited to ~10 mol% APMA content. Sufficient APMA content is required to ensure gelation, which requires a minimum of three crosslinking groups per chain, and to allow for the incorporation of 2-APBA for iminoboronate formation to achieve affinity release. Characterization after dialysis, for the purification of pCB-APMA, was performed by gel permeation chromatography (GPC) and ^{1}H NMR. Results of gel permeation chromatography showed a polydispersity of 1.54, indicating a relatively consistent molecular weight distribution (**Table 2-1A**). The percentage of APMA in pCB copolymer was found to be 8.5% by integrating the peak of APMA at approximately 3.05 ppm against polymer backbone methyl proton peak at 1.00 ppm. After conjugation with either NHS-DBCO and NHS-azide, ^{1}H NMR spectrums of pCB-DBCO and pCB-azide was obtained to show peaks at 7.5 ppm and 4.1 corresponding to DBCO aromatic protons and ethylene protons of azide side chain, and their respective integration against backbone methyl proton indicated 6.95% and 7.78% of DBCO and azide conjugation. A degradable analogue of pCB-azide, labeled pCB-azide (Cl), was synthesised in the same manner with degradable crosslinker (4-chlorophenyl sulfone) azide NHS ester with an 8.5% conjugation (**Figure 2-2A**). Synthesised 2-APBA-azide crosslinker was further conjugated to pCB-DBCO where its signature acetyl methyl peak on ^{1}H NMR spectrum was identified at 2.5 ppm, corresponding to roughly 1.8% conjugation to total repeating units per chain ((**Figure 2-2B and Table 2-1B**). Therefore, all required polymers for the

formation of hydrogels were synthesized by the functionalization of pCB-APMA using carbodiimide chemistry.

For drug release assays, two distinctive hydrogels composed of pCB-APBA and pCB-APBA (Cl) were formed by reacting pCB-(2-APBA)-DBCO with either pCB-azide, for non-degradable hydrogels, or pCB-azide (Cl), for degradable hydrogels. Both hydrogels were tested on their in-situ gelation time and recorded as approximately 17-20 minutes, respectively, which allows for the pre-mixing of polymers before injection. Injections would have to be timed to ensure in situ gelation occurs. Therefore, hydrogels for the construction of affinity and pulsatile protein delivery vehicles can be easily formed. For drug delivery, we would include the protein therapeutic prior to gelation within the pCB-(2-APBA)-DBCO solution (**Figure 2-2C**).

2.2.2 Synthesis of oxyaminated bevacizumab (Oxy-Bv) conjugates

Although iminoboronates can be formed with amine groups on the protein therapeutic, we also synthesised oxyaminated Bv (Oxy-Bv) to increase the strength of the interaction (**Figure S4**); the bioactivity of Oxy-Bv was determined to be similar to Bv as described below. The number of oxyamine conjugates on Bv was determined by MALDI-TOF/TOF (**Figure S3**). Oxyaminated bevacizumab, or Oxy-Bv, was synthesised with EDC-NHS conjugation at surface carboxylate groups, and the number of conjugations was summarised in Table S1. Molecular weight of Oxy-Bv obtained from MALDI-TOF mass spectrometry reported a mass increase of 2.03 kDa compared to native, which corresponded to an average of approximately 23 O, O'-1, 3-Propanediylbishydroxylamine molecules conjugated on Bv surface. The higher affinity of oxyamines (K_d~10^{-5} M) compared to amines (K_d~10^{-3} M) for the formation of iminoboronates may result in slower release profiles [65,66].

A

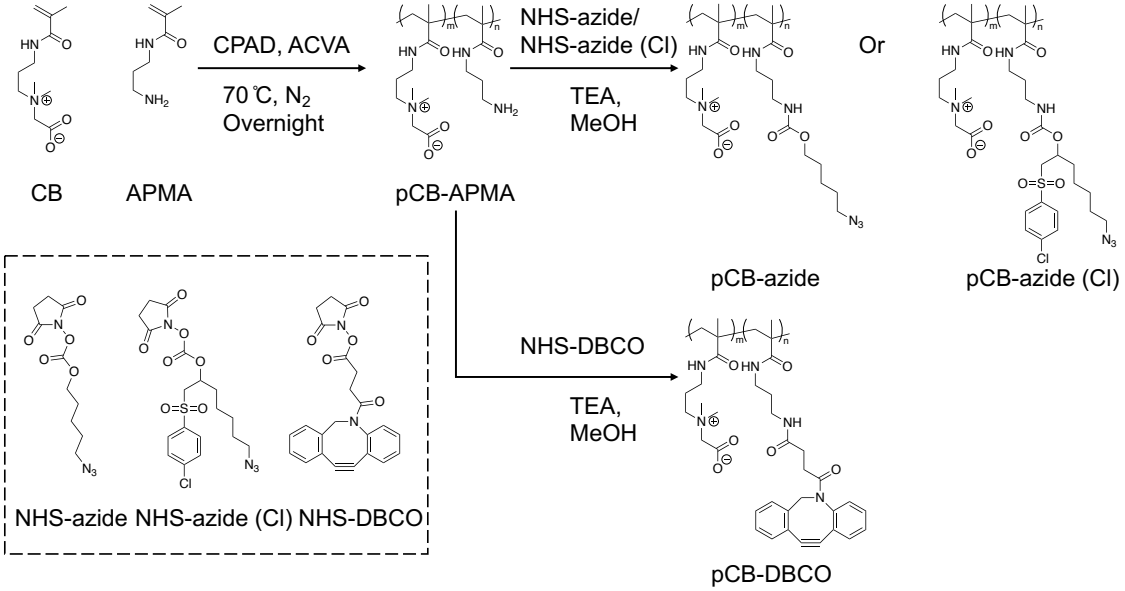
CPAD, ACVA
70 ℃, N2
Overnight
NHS-azide/
NHS-azide (Cl)
TEA,
MeOH
Or
CB
APMA
pCB-APMA
pCB-azide
pCB-azide (Cl)
NHS-DBCO
TEA,
MeOH
NHS-azide NHS-azide (Cl) NHS-DBCO
pCB-DBCO

B

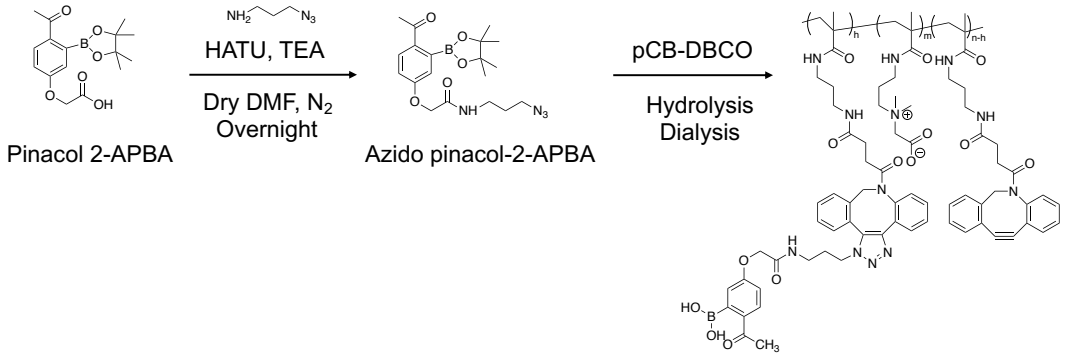
HATU, TEA
Dry DMF, N2
Overnight
pCB-DBCO
Hydrolysis
Dialysis
Pinacol 2-APBA
Azido pinacol-2-APBA
pCB-(2-APBA)-DBCO

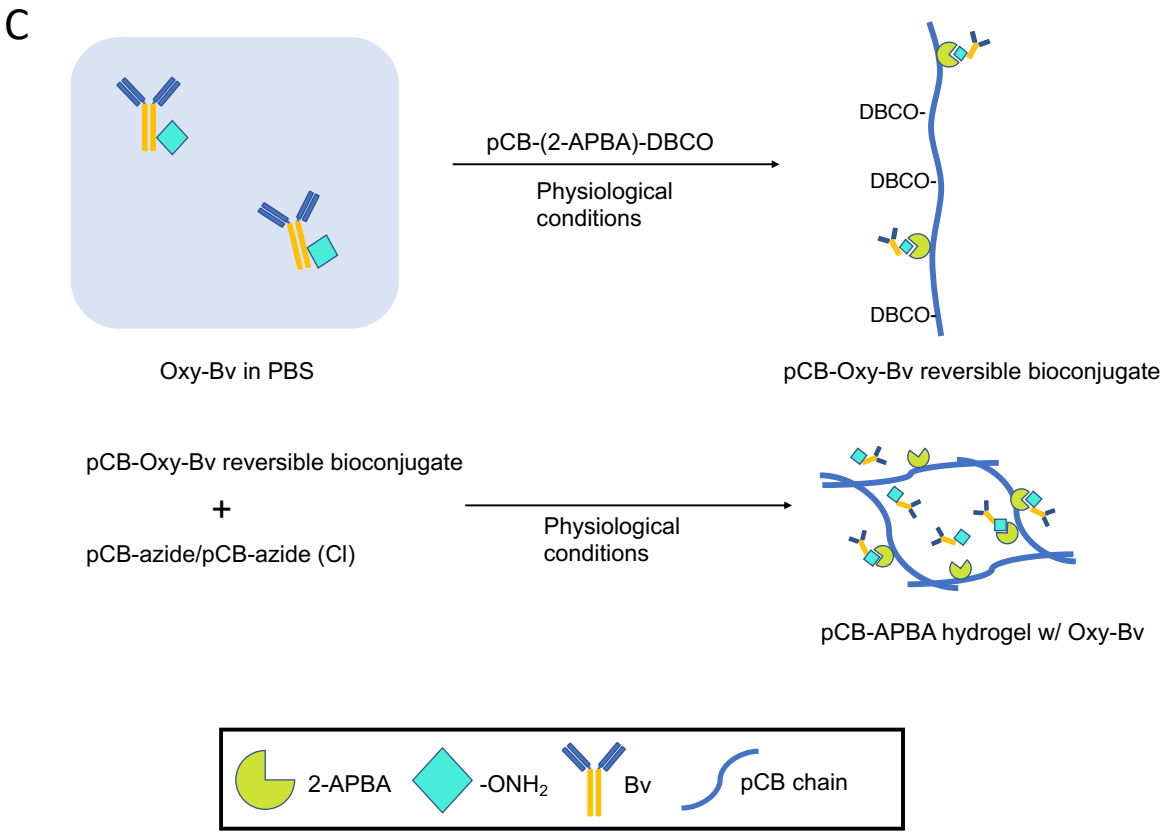

Figure 2-2. Synthesis of pCB-APBA hydrogels. (A) Synthesis of non-degradable pCB-azide, degradable pCB-azide (Cl), and pCB-DBCO. (B) Synthesis of pCB-(2-APBA)-DBCO via partial conjugation of 2-APBA onto pCB-DBCO. (C) Gelation schematic of pCB-APBA hydrogel with Oxy-Bv model therapeutic. An alternative pCB-APBA hydrogel was created with native Bv instead of Oxy-Bv to achieve distinctive release profiles (**Figure 2-3**). All reactions occurred in aqueous solution at room temperature and under atmospheric conditions unless otherwise specified.

Table 2-1. **Synthesis of pCB hydrogel component (A) Molecular weight distribution of pCB-APMA, and (B) Percent sidechain conjugation to pCB polymer**

(A) Molecular weight distribution of pCB-APMA

Polymer Name	Mn (kDa)	Mw (kDa)	Dispersity
pCB-APMA	23	35	1.54

(B) Percent conjugation of pCB polymer

Polymer Name	Reactive group	mol% reactive monomer
pCB-APMA	Primary amine	8.5
pCB-azide (non-degradable linker)	Azide	7.8
pCB-azide (degradable linker)	Azide	8.5
pCB-DBCO	DBCO	6.9
pCB-(2-APBA)-DBCO	2-APBA and DBCO	2.0

2.2.3 Native and oxyaminated bevacizumab exhibited distinctive release profiles

Release assays of Bv or oxy-Bv was performed using 10% wt. pCB-APBA hydrogels in PBS with 0.05% wt. BSA; the presence of BSA provides a competitive environment for the therapeutic protein with hydrogel binding sites. The hydrogel was loaded to a final concentration of either 5 μg/ml and 25 μg/ml native Bv and oxyaminated bevacizumab, or Oxy-Bv. A reversible covalent bond was subsequently formed between antibody surface amines or conjugated oxyamine moieties with immobilised 2-APBA on polymer sidechain. An initial burst release between 40% to 57% was observed in the first 24-36 hours, followed by short-term sustained release that eventually plateaued after two weeks (**Figure 2-3**). At both concentration conditions, Oxy-Bv demonstrated significantly slower release rates compared to native Bv, which was close to 100% depleted from hydrogel towards the end of Week 2. This result was consistent with greater iminoboronate lifetimes, as reported in the literature, when formed between conjugated oxyamine moieties and 2-APBA on hydrogel backbone. Therefore, to achieve pulsatile release, we will

require the use of oxy-Bv and not Bv, as Bv is completely released even without hydrogel degradation.

By plotting remaining Bv concentration against time, a post-burst effective first order release kinetics were observed after burst release. Specifically, linear relationship between natural logarithms of remaining bevacizumab concentration and time indicated that apparent release kinetics followed first order characteristics in Week 1 (**Figure S5**). Effective equilibrium dissociation constant K_{eff} was calculated during the phase of sustained release after Day 1, and at both concentration conditions native Bv (K_{eff}=0.30-0.38, R^2=0.996) exhibited higher calculated dissociation constants than that of Oxy-Bv (K_{eff}=0.070-0.099, R^2=0.920), indicating a reduced dissociation rate of iminoboronate formed between oxyamine moieties and 2-APBA. In summary, distinctive iminoboronate stability from protein surface modifications can be exploited to tailor respective release profiles to specific dosing requirement.

The iminoboronate affinity system developed here, the first report for a local delivery device, allows for affinity release of proteins with modification (e.g., Bv) over the course of ~1 week. Using the developed polymers, unmodified proteins can be easily added and delivered without further steps required, which was previously only possible for proteins that have inherent binding interactions with biopolymers, such as heparin binding proteins. Beyond developing a pulsatile release system, the iminoboronate affinity release mechanism can also allow for sustained release of proteins over 1 week.

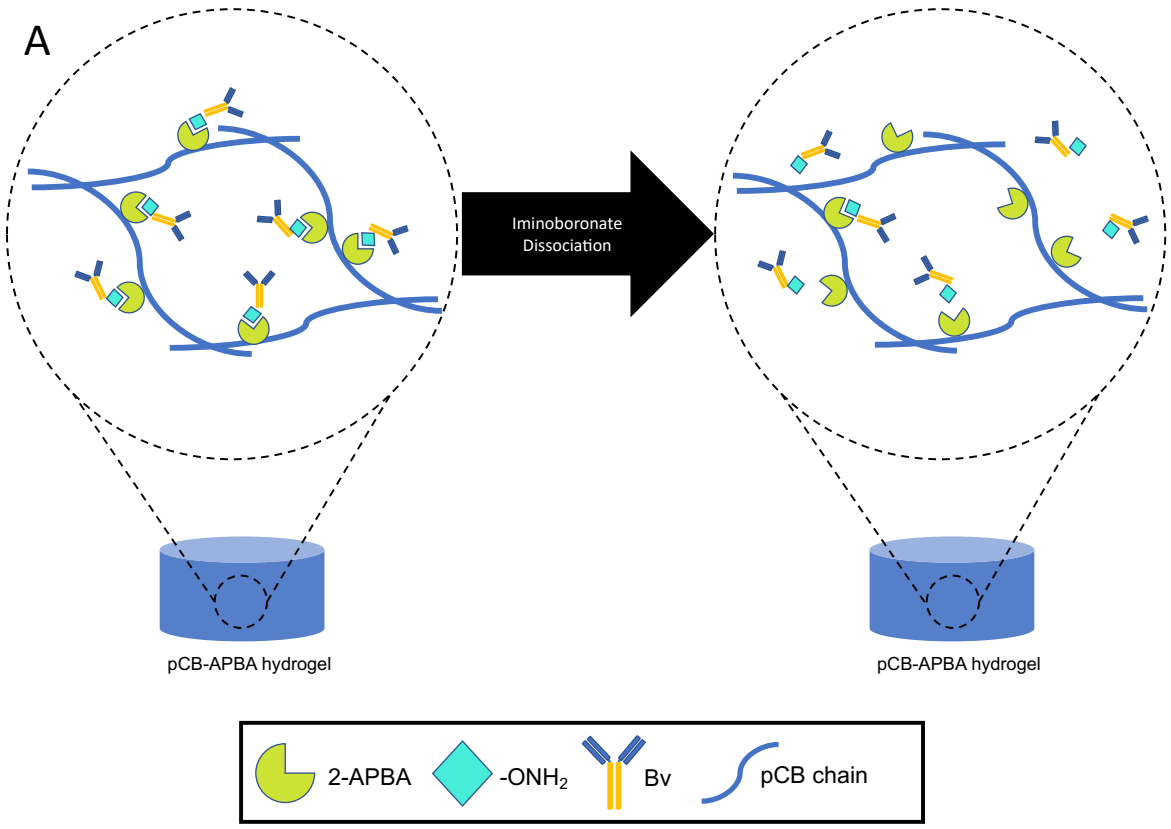

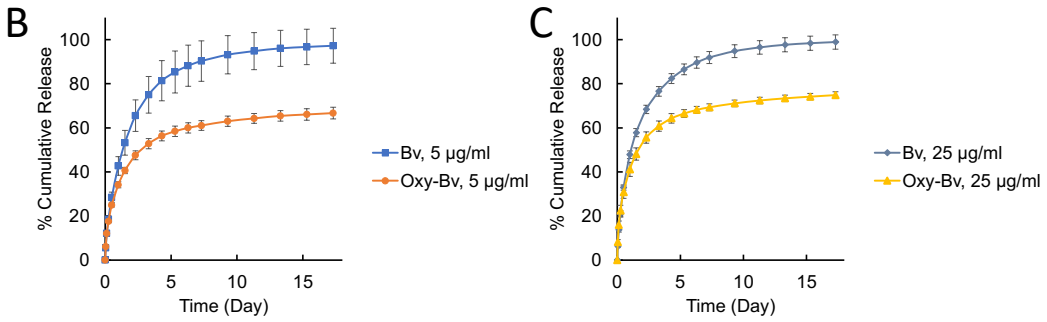

Figure 2-3. Controlled release of Bv and oxy-Bv from pCB-APBA hydrogels. (A) Schematic of Oxy-Bv released from pCB-APBA hydrogel due to iminoboronate dissociation. Alternatively, instead of Oxy-Bv, unmodified Bv was also released from pCB-APBA hydrogel following similar mechanism. Percent cumulative release of (B) 5 μg/ml of Bv and Oxy-Bv, and (C) 25 μg/ml of Bv and Oxy-Bv was determined. In both concentration conditions, Oxy-Bv exhibited slower burst and sustained release rate than Bv resulting from greater stability of iminoboronate bonds formed between 2-APBA and conjugated oxyamine groups. Therapeutic release plateaued after two weeks, with near 100% depletion of Bv from the hydrogel, while 25-33% of Oxy-Bv remained encapsulated at the end of Week 2 with minimal daily release.

2.2.4 Tunable release via fructose-induced iminoboronate dissociation

The ability to easily tune release profiles without the need for hydrogel or therapeutic modification is advantageous to identify and achieve efficacious release profiles. Moreover, tunable release is desirable for affinity-based drug release systems to accommodate a wide range of therapeutic windows. Fructose-induced dissociation of iminoboronate bond, which was previously reported in literature, presented an opportunity to design a release system that would increase the release rate of proteins in the presence of fructose[63,79]. Following the established experiment setup, 5 μg/ml of native (Bv) and oxyaminated bevacizumab (Oxy-Bv) was first encapsulated in 10% wt. pCB-APBA hydrogels in a dark 96-well plate. Subsequently, supernatant containing fructose was added on top of each well and replenished at given time intervals. Under both conditions, presence of fructose resulted in heightened burst release, indicating greater degree of dissociate between hydrogel backbone and encapsulated antibodies (**Figure S6A-B**). However, the trajectory of increased release rate did not continue beyond Day 1, suggesting a more limited impact of fructose on sustained release rate that appeared to be determined predominantly by the more stable iminoboronate bonds between Oxy-Bv and pCB backbone (**Figure S6C**). This result is expected, as fructose will alter the apparent K_D, which is known to change the initial burst with little effect on release rates after the burst.

Fructose concentration dependency of protein release rate was further demonstrated by creating pCB-APBA hydrogel in stock fructose buffer at various concentrations, which allows for fructose to be present in the gel from the beginning. For this tunable fructose displacement assay, Oxy-Bv was chosen as the model therapeutic due to a slower baseline release rate and thus could potentially offer a wider range of tunability. 5 μg/ml Oxy-Bv was encapsulated in 10% pCB-APBA hydrogel with initial concentrations of 0, 13.25, and 66.25 mM fructose. Fructose-free supernatant

was regularly replenished and the amount of released Oxy-Bv was measured the same way as previous sections. An accelerated burst release was recorded amongst fructose-loaded hydrogels, and a range of burst percent release from 40% no-fructose baseline to 58.8% was recorded in the first 36 hours proportionate to initial fructose concentrations (**Figure 2-4**). On the other hand, protein release rate after initial 36 hours followed similar kinetics across all fructose concentrations, suggesting a more limited role of fructose during sustained release. Diminishing impact of fructose after burst release is likely from fructose diffusion from the hydrogel.

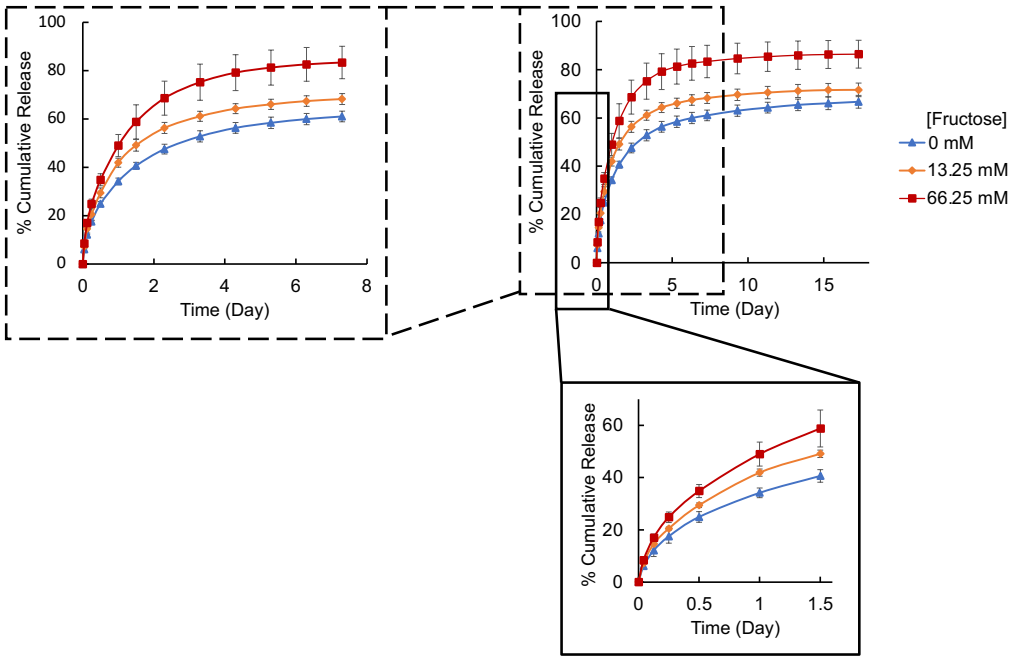

Figure 2-4. Release rate of Oxy-Bv is dependent on hydrogel fructose concentration. 5 μg/ml Oxy-Bv was reversibly immobilized in pCB-APBA hydrogel loaded with initial concentrations of fructose as listed. Subsequently, fructose-free release buffer (PBS w/ 0.05% wt. BSA) was replenished at regular interval to monitor the release of antibodies. Greater concentrations of fructose corresponded to a larger burst release rate. Overall, cumulative release of Oxy-Bv eventually plateaued after two weeks.

2.2.5 Hydrogel degradation

Degradable pCB-APBA hydrogel was created by mixing pCB-APBA-DBCO and degradable pCB-azide (Cl) at 10% wt. in PBS w/ 0.05% BSA. Hydrogel degradation was

determined by measuring the % mass of remaining hydrogel at given time intervals (**Figure S7**). Supernatant was removed and replenished the same way as release assays to maintain a steady state for continuous degradation.

2.2.6 Hydrogel degradation enabled bi-phasic, pulsatile therapeutic release

A tunable, bi-phasic pulsatile release system was developed using the degradable pCB-ABPA (Cl) hydrogel in combination with iminoboronate controlled release. The pulsatile system was developed, as a proof-of-concept, using the higher affinity oxy-Bv as Bv would result in 100% protein release without the need for hydrogel degradation. A hydrogel with a degradation timeline of greater than 2 weeks was selected to demonstrate pulsatile release. Following the established methods as previously stated, 5 μg/ml Oxy-Bv was incapsulated within 10% wt. degradable pCB-APBA (Cl) containing an initial loading of 0, 13.25, and 66.25 mM fructose, respectively. Three distinctive release profiles were observed during a month-long period, each demonstrating two separate phases of burst release (**Figure 2-5**).

During the first two weeks, Oxy-Bv release profile followed a similar trend previously established in our non-degradable hydrogel, where greater fructose level led to higher burst release of Oxy-Bv, followed by a short-term sustained release on Week 1 that largely plateaued in the second week (**Figures 2-4 and 2-5A-B**). However, unlike the previous release assays on non-degradable hydrogel, release rate of Oxy-Bv began to rise again on Day 17, initiating the second burst that eventually led to the depletion of encapsulated protein and complete gel disintegration on Day 28-32 (**Figure 2-5B-C**). Regardless of fructose concentration, degradation of pCB-APBA (Cl) hydrogel was consistent and thus timing of the second burst was largely uniform across fructose conditions (**Figures 2-5C and S7**), indicating the timing of the second burst release is likely solely controlled by the degradation rate of the hydrogel.

Overall, tunable release via iminoboronate dissociation enabled both bursts to be tailored by pre-loading specific fructose concentrations. Because the initial burst occurred prior to any significant hydrogel degradation, the release profile followed similar kinetics to that of non-degradable pCB-APBA hydrogel and was predominantly controlled by reversible iminoboronate bonding and its fructose-induced dissociation. Unlike the initial burst, the second burst release phase was caused by hydrogel crosslinker hydrolysis and thus not directly associated with iminoboronate kinetics. Instead, the release rate of the second burst was shown to be proportional to remaining Oxy-Bv concentrations, where slower initial burst corresponded to increased second burst due to greater amount of Oxy-Bv remaining encapsulated (**Figure 2-5C**).

Compared to existing non-stimuli systems such as PLGA-based microparticles, the combination of affinity release and degradable allow for the production of hydrogel-only pulsatile systems for proteins and potentially greater versatility of PLGA-hydrogel composites by incorporating an additional pulse. A highly tunable nature can be favourable for a variety of clinical practices, especially drug delivery and single-injection vaccination. Moreover, single formulation enables streamlined manufacturing processes as well as lowers complexity of transportation and storage facilities, hence further reducing associated cost and infrastructure requirement for distribution and administration.

Unlike external stimuli pulsatile systems, the hydrogel-only system will not result in bursts that occur within a few minutes or hours. Instead, the hydrogel-only system, like PLGA systems, will result in release over a few days for each burst. Therefore, hydrogel-only or hydrogel-PLGA composite systems will be most useful for regimes that benefit for multiple pulsed releases with sustained release. For Bv clinical applications, the hydrogel-only system can minimize intravitreal injections for the treatment of retinal degenerative diseases. For vaccine applications, sustained

release for each dose has been shown to improve efficacy in pre-clinical models. Hydrogel-only or hydrogel-only may therefore prove useful for a wide range of protein therapeutics.

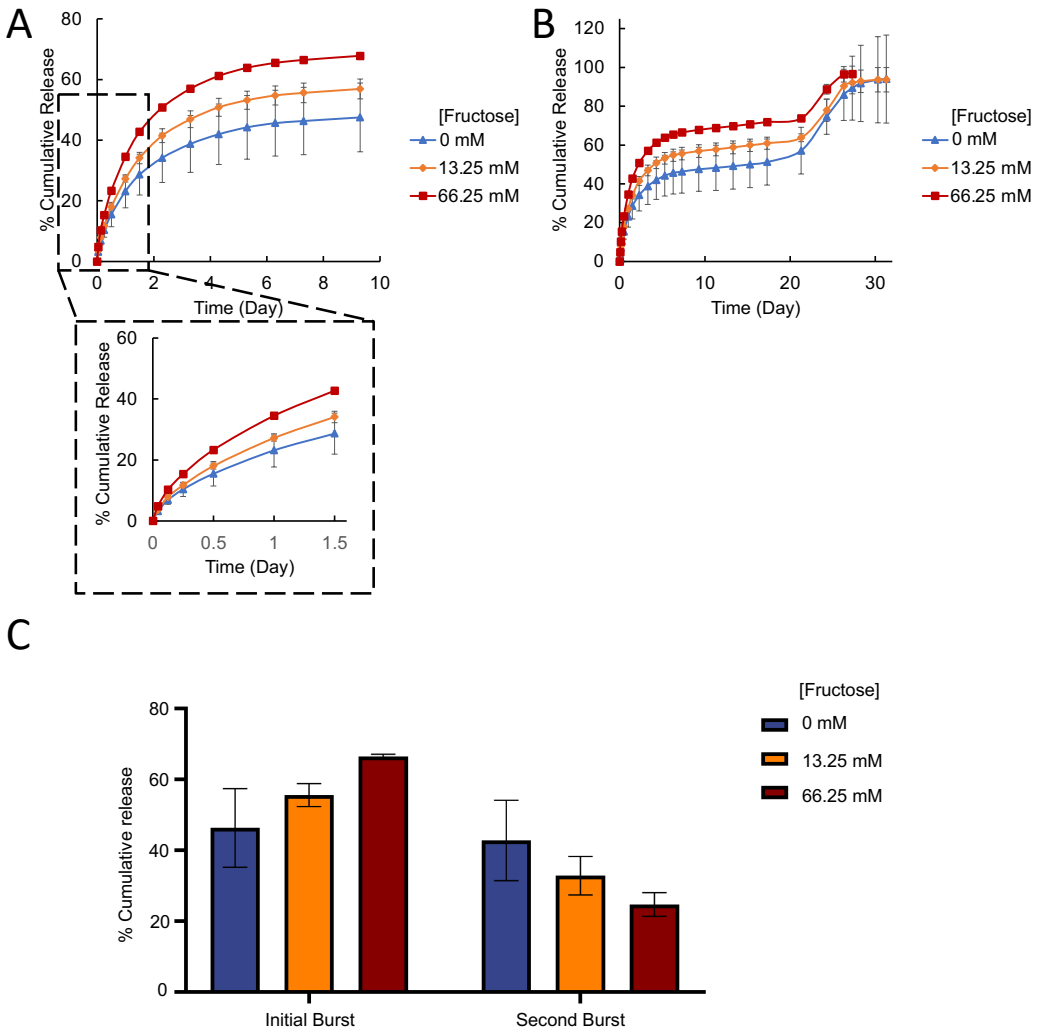

Figure 2-5. Fructose-loaded degradable hydrogels resulted in tunable and pulsatile release of Bv. Release of Oxy-Bv (5 μg/ml) from a degradable pCB-APBA hydrogel loaded with initial fructose concentrations of 0, 13.25, or 66.25 mM was followed over time. (A) Quantification of the first burst release controlled by the iminoboronate system. (B) Quantification of first and second burst release over 30 days. (C) Percent release of both initial and second bursts at given fructose concentration to demonstrate tunability. The period between two bursts was controlled by hydrogel degradation kinetics as demonstrated in **Figure S7**.

2.2.7 Oxy-Bv was bioactive according to the HUVEC proliferation assay

Bv is a human recombinant IgG with strong affinity towards pro-angiogenesis factor VEGF-165 (VEGF), thus preventing receptor binding of the latter and endothelial cell proliferation[80]. Bioactivity of Oxy-Bv was demonstrated through its inhibitory capacity against VEGF using human umbilical vein endothelial cells, or HUVEC, proliferation assay. Optimal VEGF concentration for HUVEC proliferation was first determined from a rhVEGF-165 dose response assay (**Figure 2-6A**). Passaged HUVEC cells were cultured in endothelial basal media with VEGF-165 at concentrations from 1.55 to 400 ng/ml for 4 days, and subsequently cell proliferation was determined by measuring viability using a fluorescence metabolic assay (AlarmaBlue). Among all concentration conditions, 200 ng/ml VEGF and above demonstrated maximum growth and was hence used in Bv and Oxy-Bv inhibition assay. The inhibitory effect of bevacizumab derivatives was investigated by measuring HUVEC cell growth at the presence of Bv or Oxy-Bv at varying concentrations (**Figure 2-6 B**). Overall, Oxy-Bv exhibited comparable inhibitory proliferation effects to unmodified Bv for all studied sample concentrations, indicating the oxyamine modification of Bv had minimal effect on bioactivity. In summary, oxyamine modifications on Bv did not demonstrate negative impact on its bioactivity in inhibiting HUVEC growth.

2.2.8 Cytokine release assay for the pCB-APBA hydrogel vehicle

Cytokine release assay (CRA) is an FDA-recommended method to assess therapeutic immunogenicity. Inflammatory markers IL-6, TNF-α, and IFN-γ concentrations in whole blood were assessed by ELISA for pCB-APBA hydrogel delivery system, while PBS and LPS were included as negative and positive controls, respectively (**Figure 2-6C-E**). After incubating with respective samples for 24 hours at 37 °C, blood cells were separated from plasma via centrifugation.

Presence of pCB-APBA hydrogel in blood samples demonstrated minimal inflammatory responses, as very low concentrations of pro-inflammatory cytokines were detected in blood samples with pCB-APBA across the board. In addition, in all three conditions pCB-APBA hydrogel did not show significant difference between those with PBS. On the other hand, samples with PBS and pCB-APBA hydrogel all demonstrated significantly lower cytokine levels than LPS across all three conditions. LPS is a common component of bacterial cell membrane and known to induce generation of TNF-α and IL-6 from macrophages via interaction with CD-14 membrane receptor[81]. LPS was shown to increase IL-6 and TNF-α levels by a large margin in blood, though only a small increase of IFN-γ was observed. Because no significant difference between PBS and the pulsatile drug delivery vehicle developed here, the likelihood for deleterious immune responses after implantation is low.

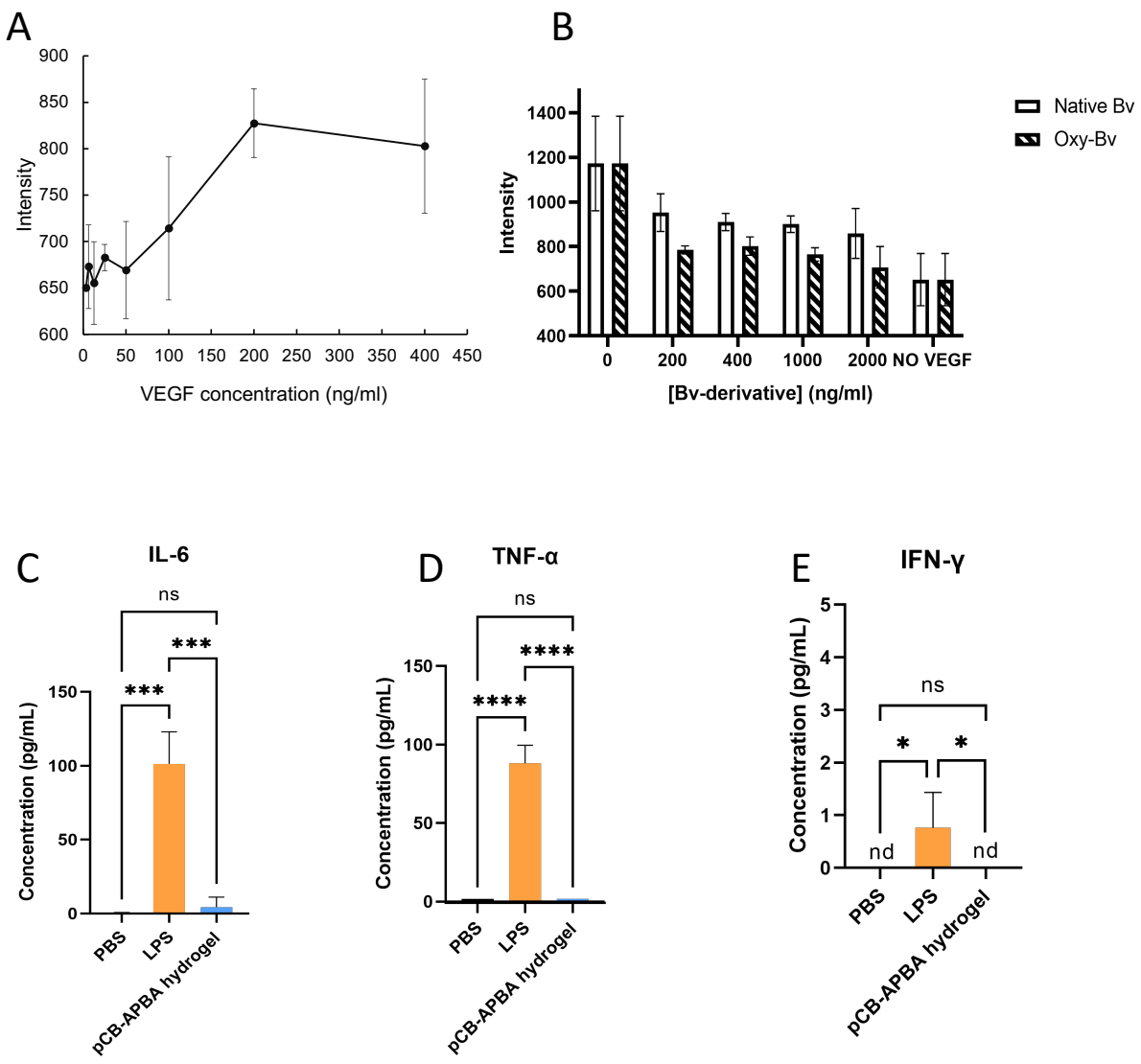

Figure 2-6. Bioactivity of Oxy-Bv and CRA of the pCB-APBA delivery system. Oxy-Bv bioactivity was tested with HUVEC cell proliferation assay by measuring cell viability with the AlarmaBlue™ fluorescence intensity at 530/590. (A) HUVEC dose response to VEGF concentration. (B) Oxy-Bv exhibited comparable bioactivity to native Bv for the inhibition of HUVEC proliferation. The cytokine release assay of the pCB-APBA hydrogel was performed in whole blood to evaluate biocompatibility. pCB-APBA hydrogel was incubated with whole blood for 24 hours at 37 °C, and pro-inflammatory cytokines (C) IL-6, (D) TNF-α, and (E) IFN-$\boldsymbol{\gamma}$ levels

were measured by ELISA. PBS and LPS were included as negative and positive controls, respectively (nd = non-detectable; ns= $p > 0.05$ *= $p < 0.05$; ***= $p < 0.001$; ****= $p < 0.0001$).

2.3 Further Discussion

The delay between the two burst releases can be tuned by altering the degradation kinetics of the hydrogel. The crosslinker used in this study incorporates an electronically tuned hydrolytic carbamate bond, where the electron withdrawing group alters the rate of degradation. For example, the use of a weaker electron withdrawing group will slow hydrogel degradation and delay the second bursts release. Therefore, the timing of the burst releases can be tuned by altering the crosslinker electron withdrawing group.

Although this is the first demonstration of a hydrogel-only pulsatile release system without the need for an external stimulus, it is limited to two pulses of protein release. If more release pulses are required, we can explore the inclusion of PLGA microparticles. The hydrogel would therefore expand the potential of PLGA systems by improving localization and providing two additional release pulses.

2.4 Conclusion

The combination of affinity-like release and controlled hydrogel degradation allows for the fabrication of hydrogel-only vehicles for tunable pulsatile release of proteins. Through a combination of iminoboronate chemistry and controlled hydrolysis of hydrogel crosslinks, tunable release with only single polymer formulation, hence reducing complexity in manufacturing and alleviating pressure on the logistics of administration, was developed. Moreover, the iminoboronate affinity delivery system provides a platform for sustain release of unmodified proteins over 1 week. Furthermore, zwitterionic pCB-APBA hydrogel demonstrated minimal immunogenicity according to the CRA. Therefore, the hydrogel-only system can help expand sustained and pulsatile release applications for protein therapeutics.

2.5 Materials and Methods

2.5.1 Materials and instruments

O,O'-1,3-Propanediylbishydroxylamine, 4,4-azobis(4-cyanovaleric acid), 4-cyano-4-(phenylcarbonothioylthio)pentanoic acid, N-Hydroxysuccinimide (NHS), bovine serum albumin (BSA), and lipopolysaccharide (LPS) were obtained from Sigma-Aldrich (Oakville, ON). Alexa Flour 488 NHS ester, AlarmaBlue reagent, and Invitrogen eBioscience ELISA kits for IL-6, TNF-α, and IFN-γ were obtained from Thermo Fisher Scientific (Burlington, ON). DBCO-NHS and azide-NHS esters were purchased from Click Chemistry Tools (Scottsdale, AZ). N-(3-aminopropyl)methacrylamide hydrochloride (APMA-HCl) was purchased from Polysciences Inc. (Warrington, PA). 1-ethyl-3-(3-dimethylaminopropyl)carbodiimide hydrochloride (EDC-HCl) was purchased from Chem-Impex International Inc. (Wood Dale, IL). Dialysis tubes were purchased from Repligen Spectrum Laboratories (Rancho Dominguez, CA). Human rhVEGF-165 was purchased from Biolegend (San Diego, CA). Endothelial Cell Growth Media 2 (EGM 2) was purchased from Promo Cell (Heidelberg, Germany). HUVEC cells were purchased from Angio-Proteomie (Boston, Massachusetts). HATU was a gift from Adronov Lab at McMaster University. Bevacizumab was obtained from Boston Children's Hospital Pharmacy. Degradable azide (Cl)-NHS crosslinker came from the stock that had been previously synthesised in Wylie Lab[67].

2.5.2 Synthesis of azido pinacol 2-acetyl phenylboronate ester

One molar equivalence of 3-azido propanamine, 2-acetyl, 4-oxyacetate pinacol phenylboronate ester (pinacol-protected 2-APBA) and HATU was mixed in a reactor subsequently filled with nitrogen, and then dissolved in DMF to a concentration of 0.125 M. The reaction mixture was incubated for 30 minutes before adding in a further 25% volume percent 1.56 M

triethylamine in DMF. Reaction was stirred at room temperature overnight. Structure of pinacol-protected azido 2-APBA was analysed with ^{1}H NMR spectrum at Supplement Figure. 3.

2.5.3 Synthesis of carboxybetaine (CB) monomer

Carboxybeteine monomers were synthesised with an established protocol[60]. In summary, 7.75 grams (45.52 mmol) of N-(3-dimethylaminopropyl) methacrylamide was first dissolved in 100 mL dry acetonitrile under nitrogen, with 10 grams (5.57 mL) t-butyl acetate added dropwise. Subsequently, the reaction mixture was heated to 50 °C and kept overnight. The product, t-butyl protected carboxybetaine monomer, was precipitated in 250 mL cold dimethyl ether and washed out with an additional 100 mL before drying overnight under vacuum. To remove t-butyl protection group, 6 grams of protected monomer was mixed with 5 mL of trifluoroacetic acid and left overnight. The reaction mixture was then precipitated and washed in 50 mL diethyl ether, dissolved in H_2O, and finally lyophilised to yield eprotected monomer product.

2.5.4 Poly(carboxybetaine-co-aminopropyl methacrylamide) copolymer synthesis

Poly(carboxybetaine-co-aminopropyl methacrylamide) copolymer, or pCB-APMA, was synthesized from previously published protocol[60]. In summary, 1.5 grams of carboxybetaine (CB) and 30.03 mg APMA monomers were dissolved in 4.778 ml acetate buffer. Additional 4.287 mg of chain transfer agent 4-Cyano-4-(phenylcarbonothioylthio)pentanoic acid and 0.859 mg 4,4′-azobis(4-cyanovaleric acid) initiator were first dissolved in 0.434 ml dioxane and subsequently mixed with CB and APMA monomer solution. Subsequently the pH of reaction mixture was adjusted to 3-4, transferred into a Schlenk flask, and purged with nitrogen using a “freeze-pump-thaw” method. Polymerisation was carried out in 70 degrees oil bath overnight for a total of approximately 16 to 20 hours, and the reaction mixture was dialysed against 5 litres of water with 5 ml 1M HCl for two days. Purified sample was lyophilised and analysed with gel permeation

chromatography (GPC) and ^{1}H NMR for molecular weight, dispersity, and percent sidechain substitution.

2.5.5 Synthesis of copolymers pCB-azide, pCB-azide (Cl), pCB-DBCO, and pCB-(2-APBA)-DBCO

Synthesis of pCB-azide, and pCB-DBCO was performed according to previously established protocol (**Figure S1**)[43]. For each batch of pCB-Az or pCB-DBCO, 386 mg of pCB-APMA copolymer was dissolved in 5 ml methanol with 27 mg of azide-NHS or 38 mg of DBCO-NHS esters respectively. 50 μl of triethylamine was added into the reaction mixture dropwise. Reaction was carried out under nitrogen at room temperature overnight, after which the sample would be precipitated in 45 ml of diethyl ether and subsequently dried in vacuum oven at 60 degrees Celsius. The degradable pCB-azide (Cl) polymer was synthesised following the same method but with the degradable azide (Cl)-NHS crosslinker. Further modification on pCB-DBCO was carried out by conjugating 2-acetyl phenylboronic ester azide. Specifically, 319 mg pCB-DBCO was dissolved in 2380 μL water alongside 2.8 mg pinacol-protected 2-APBA-azide and incubated overnight, then precipitated in diethyl ether, dried, and dissolved in water. The polymer solution was then extracted with dichloromethane and dialysed for two days with water changed twice a day. The dialysis process also served to remove protective pinacol groups from conjugated 2-APBA via hydrolysis[82]. Purified sample was lyophilised and analysed with ^{1}H NMR.

2.5.6 Analysis of polymer molecular weight distribution

Molecular weight and dispersity of pCB-APMA polymers were characterised with gel permeation chromatography (GPC) using Agilent 1260 Infinity II LC system with Superose 6 10/300 Increase GL column. Polymer sample was run in PBS with 0.05% wt. sodium azide at 1

ml/min and monitored via refractive index (RI). Molecular weight distribution was determined with a calibration curve generated from a series of poly(ethylene glycol) (PEG) standards.

2.5.7 Gelation time of pCB gels

10% weight percent of pCB-Az, pCB-Az (Cl), and pCB-(2-APBA)-DBCO was first dissolved in PBS separately and then mixed in a 2 ml glass vial. The glass via was tilted regularly to monitor solidity or viscosity of gel mixture, and subsequently the time of sol-gel transition was recorded as gelation time.

2.5.8 Bevacizumab modification with O,O'-1,3-Propanediylbishydroxylamine dihydrochloride

The method of conjugating bevacizumab surface carboxylate group to O, O'-1, 3-Propanediylbishydroxylamine was based upon established protocols[83,84]. Bevacizumab was diluted to a concentration of 0.033 mM in MES buffer, pH=6.0, where EDC and NHS ester were first dissolved at concentrations of 50 mM and 75 mM respectively. This reaction mixture was incubated for 40 minutes before O, O'-1, 3-Propanediylbishydroxylamine dihydrochloride was added to the concentration of 6.7 mM. The reaction mixture was incubated overnight at room temperature, desalted through buffer exchange, and analysed via MALDI-TOF/TOF on positive mode. Unmodified bevacizumab was used as reference to measure mass increase after conjugation with O, O'-1, 3-Propanediylbishydroxylamine.

2.5.9 Bevacizumab labelling using Alexa Fluor 488 (AF-488) NHS ester

Bevacizumab-oxyamine conjugates and native bevacizumab were labeled with Alexa Fluor 488 NHS ester. Briefly, 0.8 μL AF-488 NHS ester stock (10 mg/ml in dry DMF) was added to in PBS and incubated overnight. Labeled bevacizumab was subsequently dialysed in PBS at 4 ˚C in

the dark for three days, with buffer changed twice a day. The degree of labelling (DOL) was determined using NanoDrop™ OneC Microvolume UV-Vis Spectrophotometer.

2.5.10 Protein release assay with native and oxyamine-modified bevacizumab

AF-488 labelled oxyamine-modified bevacizumab (Oxy-Bv) was incubated overnight with 120 µl 10% wt. pCB-(2-APBA)-DBCO in PBS with 0.05% wt. BSA at 5 and 25 µg/ml respectively, and then mixed with an equal amount of 10% wt. pCB-Az to form pCB-(2-APBA) hydrogel. Respective controls were created by repeating the same process with AF-488 labelled native bevacizumab (Bv). For every therapeutic concentration, gels were casted in quadruplets totalling 60 µl each in a black 96-well plate. After setting in dark for an hour, 200 µl PBS with 0.05% wt. BSA was added on top each gel and incubated at 37 °C for a further hour. Subsequently, buffer on top of hydrogel, aptly labelled "supernatant", was taken out at given interval while fresh supernatant was replenished. Supernatant readings were taken at a Biotek Cytation 5 plate reader (ex. 495 nm, em. 519 nm, gain=134), where bevacizumab concentration was determined using a calibration curve made from a series of stocks at known concentrations.

2.5.11 Fructose-mediated protein release assays

To determine whether incorporation of fructose could facilitate faster release rate, a supernatant made composed of PBS with 0.05% wt. BSA and 5.3 mM fructose was added on top of 10% wt. pCB-(2-APBA) hydrogels containing 5 µg/ml native or oxyamine-modified bevacizumab. The supernatant was removed and replenished at set time intervals, where concentration of released antibodies was determined via fluorescence reading as elaborated in Section 9.

Further investigation on tunability of Oxy-Bv release profile through fructose concentration gradient led to direct incorporation of fructose into pCB-APBA hydrogel. In summary, 10% wt.

pCB-APBA hydrogel was formed in PBS, 0.05% wt. BSA containing 0 mM, 13.25 mM, and 66.25 mM fructose. Simultaneously, Oxy-Bv was loaded at the initial concentration of 5 μg/ml. Following the same steps as previously stated, supernatant was constantly removed and replenished from the 96-well plate, but in this assay the supernatant contained no fructose to simulate generic physiological conditions. Concentration of released antibody was determined via fluorescence reading established in Section 9.

2.5.12 Hydrogel degradation and pulsatile release

Degradable pCB-APBA hydrogels were fabricated by crosslinking the degradable pCB-azide (Cl) with pCB-APBA-DBCO at 10% wt. in PBS w/ 0.05% BSA. Hydrolytic degradation kinetics was tested by incubating in PBS w/ 5% BSA at 0 and 66.25 mM fructose concentrations at 37 °C and 5% CO_2. Subsequently, PBS w/ 5% BSA supernatant was replenished and removed at given time intervals on top of hydrogels and the remaining mass was recorded to illustrate swelling and crosslinker hydrolysis (**Figure S7**).

Release assays with tunable and pulsatile characteristics was performed by replacing nondegradable pCB-APBA hydrogel from previous assays with a degradable equivalence, pCB-APBA (Cl) hydrogel using pCB-azide with degradable crosslinker and pCB-APBA-DBCO. All other materials, conditions, and experiment procedures were prepared identical to that described in the preceding section.

2.5.13 HUVEC cell proliferation assay

Bioactivity of Oxy-Bv was studied by conducting HUVEC cell proliferation assays based on previous tests on native bevacizumab[85]. A VEGF dose response curve was constructed by measuring HUVEC proliferation with a series of rhVEGF concentration (**Figure 2-6A**). VEGF was serially diluted 8-fold from 400 ng/ml stock to 1.5 ng/ml in endothelial basal media (EBM)

with 2% Penstrep and no supplements. VEGF in EBM at was then added into a 96-well plate where HUVEC cells were plated at approximately 10,000 cells per well to a total of 100 μL, while EBM with no VEGF was used as a negative control. Subsequently the plate was incubated at 37 °C in 5% CO_2 for four days. On Day 4, the cells were treated with AlarmaBlue reagent at 50 μl/well for 6 hours. Fluorescence reading at 530/590 nm (Gain=50) was taken and recorded on a Biotek Cytation 5 plate reader.

To test Oxy-Bv bioactivity, in a 96-well plate HUVEC cells were plated at 10, 000 cells/well in EBM at 200 ng/ml VEGF with no supplements except for the negative control group, where no VEGF was present in the media. Native Bv and Oxy-Bv were subsequently diluted to 0, 200, 400, 1000, and 2000 ng/ml and added to the plate to a total of 100 μl per well. The plate was incubated at 37 °C in 5% CO_2 for four days, after which the cells were incubated AlarmaBlue for another 6 hours before fluorescence reading was taken.

2.5.14 Immunogenicity test

Immunogenicity of pCB-APBA hydrogel was tested using cytokine release assay (CRA) in whole blood and inflammatory markers IL-6, TNF-α, and IFN-γ were monitored for potential foreign body response against pCB-APBA[86,87]. Following previously published methods, 1 ml fresh heparinised blood was incubated with pCB-APBA hydrogel (100 μl at 10% wt.) at 37 °C for 24 hours while PBS (100 μl) and LPS (10 ng/ml, 100 μl) were included as respective negative and positive controls[43]. On the following day, blood cells were removed by centrifuging at 2000 G for 10 minutes, and isolated plasma was frozen in -80 °C until further analysis. The levels of IL-6, TNF-α, and IFN-γ in plasma were tested using eBiosciences ELISA kits according to protocols provided.

2.5.15 Statistical analysis

All release assay conditions were performed in quadruplicates and all samples in every other experiment were tested in triplicates. Standard deviation was represented using ± error bars in figures. Statistical analysis was performed by Graphpad Prism (ns= $p > 0.05$ *= $p < 0.05$; ***= $p < 0.001$; ****= $p < 0.0001$).

3 Recommended future works

3.1 *In vivo* intravitreal release of therapeutic using TaPIRS

To further investigate the therapeutic effects of controlled protein release, we propose an *in vivo* testing on intravitreal delivery of bevacizumab. Rabbit would be used as model animal in these experiments. The degradable hydrogel system can be injected using a 30G needle directly into intravitreal space where gelation occurs. Subsequently, intraocular concentration of released Bv can be measured using immunoassay, such as ELISA, where key pharmacokinetic parameters, such as clearance, volume of distribution, half-life etc., can be derived from rabbit model[88].

3.2 Alternative iminoboronate chemistry and controlled fructose release for greater range of tunability

In its current form, our affinity pulsatile release system has approximately a 20% window of tunability during its initial burst. In addition, approximately 30%-40% of Oxy-Bv was release in the first 36 hours even without added fructose. Thus, an improved range of tunability would be ideal to accommodate varying requirements in clinical applications. Hereby I propose the use of 2-formyl phenylboronic acid (2-AFBA) on pCB hydrogel for greater iminoboronate kinetic stability. Previous studies have demonstrated the dissociation constant of iminoboronate formed between 2-APBA and oxyamine groups at 10^{-9} M, compared to that of 2-APBA at 10^{-5} M[64]. Greater iminoboronate stability will likely lead to slower baseline burst release rate with no displacement release, and thus opening a greater tunability window.

Besides tailoring burst release, it is worth investigating whether greater fructose retention would demonstrate greater impact on sustained release rate. As a small molecule, it is expected for fructose to escape from hydrogel at relatively short time. However, inspired by controlled protein release mechanisms, fructose can also be directly onto pCB-azide using a dynamic crosslinker.

Consequently, fructose concentration can be better maintained within hydrogel in a similar manner to controlled protein release. Improvements on fructose retention also have the added benefit of further reducing individual hydrogel components, thus enabling even simpler storage and administration.

3.3 *In vivo* immunogenicity testing for vaccination applications

While there have been several reported pulsatile release systems for vaccination, in vivo testing of their efficacy remains inadequate. Hereby, we propose an *in vivo* testing of the tunable and pulsatile release system conducted in mice model. Specifically, model antigen ovalbumin will be loaded into the hydrogel at varying concentrations of fructose. A positive control includes two bolus injections of equivalent ovalbumin amount administered at approximately the same time, while pCB-APBA hydrogels with matching fructose concentration will be used as negative controls. Subsequently, an IgG antibody titer from mice sera will be performed on a weekly basis. Efficacy of our tunable and pulsatile release system as a vaccine delivery vehicle will be measured by peak ovalbumin Antibody levels as well as between individual data point against respective time-matched controls. Results from *in vivo* immunogenicity tests would validate the potential application in delivery protein antigens and provide valuable data to aid the design of pre-clinical trials.

4 References

1. Banks, W. A. Characteristics of compounds that cross the blood-brain barrier. *BMC Neurology* **9**, S3 (2009).
2. Miura, Y. *et al.* Cyclic RGD-Linked Polymeric Micelles for Targeted Delivery of Platinum Anticancer Drugs to Glioblastoma through the Blood–Brain Tumor Barrier. *ACS Nano* **7**, 8583–8592 (2013).
3. National Center for Immunization and Respiratory Diseases. General recommendations on immunization --- recommendations of the Advisory Committee on Immunization Practices (ACIP). *MMWR Recomm Rep* **60**, 1–64 (2011).
4. Cleland, J. Single-administration vaccines: controlled-release technology to mimic repeated immunizations. *Trends in Biotechnology* **17**, 25–29 (1999).
5. Hou, Y. *et al.* Engineering a sustained release vaccine with a pathogen-mimicking manner for robust and durable immune responses. *Journal of Controlled Release* **333**, 162–175 (2021).
6. Kaneko, Y., Sakai, K., Kikuchi, A., Sakurai, Y. & Okano, T. Fast swelling/deswelling kinetics of comb-type grafted poly(*N* -isopropylacrylamide) hydrogels. *Macromolecular Symposia* **109**, 41–53 (1996).
7. Kataoka, K., Miyazaki, H., Bunya, M., Okano, T. & Sakurai, Y. Totally Synthetic Polymer Gels Responding to External Glucose Concentration: Their Preparation and Application to On−Off Regulation of Insulin Release. *J Am Chem Soc* **120**, 12694–12695 (1998).
8. Kwon, I. C., Bae, Y. H., Okano, T., Kim, S. W. & Berner, B. Stimuli sensitive polymers for drug delivery systems. *Makromolekulare Chemie. Macromolecular Symposia* **33**, 265–277 (1990).
9. Edelman, E. R., Kost, J., Bobeck, H. & Langer, R. Regulation of drug release from polymer matrices by oscillating magnetic fields. *Journal of Biomedical Materials Research* **19**, 67–83 (1985).
10. Kim, C.-K. & Lee, E.-J. The controlled release of blue dextran from alginate beads. *International Journal of Pharmaceutics* **79**, 11–19 (1992).
11. Langer, R. New Methods of Drug Delivery. *Science (1979)* **249**, 1527–1533 (1990).
12. Jaganathan, K. S. *et al.* Development of a single dose tetanus toxoid formulation based on polymeric microspheres: a comparative study of poly(d,l-lactic-co-glycolic acid) versus chitosan microspheres. *International Journal of Pharmaceutics* **294**, 23–32 (2005).
13. Feng, L. *et al.* Pharmaceutical and immunological evaluation of a single-dose hepatitis B vaccine using PLGA microspheres. *Journal of Controlled Release* **112**, 35–42 (2006).
14. Baras, B., Benoit, M.-A. & Gillard, J. Parameters influencing the antigen release from spray-dried poly(dl-lactide) microparticles. *International Journal of Pharmaceutics* **200**, 133–145 (2000).
15. Makino, K. *et al.* Pulsatile drug release from poly (lactide-co-glycolide) microspheres: how does the composition of the polymer matrices affect the time interval between the initial burst and the pulsatile release of drugs? *Colloids and Surfaces B: Biointerfaces* **19**, 173–179 (2000).
16. Guarecuco, R. *et al.* Immunogenicity of pulsatile-release PLGA microspheres for single-injection vaccination. *Vaccine* **36**, 3161–3168 (2018).

17. Sanchez, A., Gupta, R. K., Alonso, M. J., Siber, G. R. & Langer, R. Pulsed Controlled-Release System for Potential Use in Vaccine Delivery. *Journal of Pharmaceutical Sciences* **85**, 547–552 (1996).
18. Mogi, T. *et al.* Sustained release of 17β-estradiol from poly (lactide-co-glycolide) microspheres in vitro and in vivo. *Colloids and Surfaces B: Biointerfaces* **17**, 153–165 (2000).
19. Lu, X. *et al.* Engineered PLGA microparticles for long-term, pulsatile release of STING agonist for cancer immunotherapy. *Sci Transl Med* **12**, (2020).
20. Kim, S. M., Patel, M. & Patel, R. PLGA Core-Shell Nano/Microparticle Delivery System for Biomedical Application. *Polymers (Basel)* **13**, 3471 (2021).
21. Yu, M. *et al.* Core/shell PLGA microspheres with controllable *in vivo* release profile via rational core phase design. *Artificial Cells, Nanomedicine, and Biotechnology* **46**, 1070–1079 (2018).
22. Singh, N. K. & Lee, D. S. In situ gelling pH- and temperature-sensitive biodegradable block copolymer hydrogels for drug delivery. *Journal of Controlled Release* **193**, 214–227 (2014).
23. Hoare, T. R. & Kohane, D. S. Hydrogels in drug delivery: Progress and challenges. *Polymer (Guildf)* **49**, 1993–2007 (2008).
24. Alvarez-Lorenzo, C. *et al.* Temperature-sensitive chitosan-poly(N-isopropylacrylamide) interpenetrated networks with enhanced loading capacity and controlled release properties. *Journal of Controlled Release* **102**, 629–641 (2005).
25. Ankareddi, I. & Brazel, C. S. Synthesis and characterization of grafted thermosensitive hydrogels for heating activated controlled release. *International Journal of Pharmaceutics* **336**, 241–247 (2007).
26. Bae, J. W., Go, D. H., Park, K. D. & Lee, S. J. Thermosensitive chitosan as an injectable carrier for local drug delivery. *Macromolecular Research* **14**, 461–465 (2006).
27. Rodríguez, R., Alvarez-Lorenzo, C. & Concheiro, A. Interactions of ibuprofen with cationic polysaccharides in aqueous dispersions and hydrogels. *European Journal of Pharmaceutical Sciences* **20**, 429–438 (2003).
28. Andrade-Vivero, P., Fernandez-Gabriel, E., Alvarez-Lorenzo, C. & Concheiro, A. Improving the Loading and Release of NSAIDs from pHEMA Hydrogels by Copolymerization with Functionalized Monomers. *Journal of Pharmaceutical Sciences* **96**, 802–813 (2007).
29. Nuttelman, C. R., Tripodi, M. C. & Anseth, K. S. Dexamethasone-functionalized gels induce osteogenic differentiation of encapsulated hMSCs. *Journal of Biomedical Materials Research Part A* **76A**, 183–195 (2006).
30. Sun, Y., Nan, D., Jin, H. & Qu, X. Recent advances of injectable hydrogels for drug delivery and tissue engineering applications. *Polymer Testing* **81**, 106283 (2020).
31. Singh, N. K. & Lee, D. S. In situ gelling pH- and temperature-sensitive biodegradable block copolymer hydrogels for drug delivery. *Journal of Controlled Release* **193**, 214–227 (2014).
32. Qian, Y., Wang, F., Li, R., Zhang, Q. & Xu, Q. Preparation and evaluation of in situ gelling ophthalmic drug delivery system for methazolamide. *Drug Development and Industrial Pharmacy* **36**, 1340–1347 (2010).
33. Gupta, S. Carbopol/Chitosan Based pH Triggered In Situ Gelling System for Ocular Delivery of Timolol Maleate. *Scientia Pharmaceutica* **78**, 959–976 (2010).

34. Tayel, S. A., El-Nabarawi, M. A., Tadros, M. I. & Abd-Elsalam, W. H. Promising ion-sensitive in situ ocular nanoemulsion gels of terbinafine hydrochloride: Design, in vitro characterization and in vivo estimation of the ocular irritation and drug pharmacokinetics in the aqueous humor of rabbits. *International Journal of Pharmaceutics* **443**, 293–305 (2013).
35. Han, S.-S. *et al. In situ* cross-linkable hyaluronic acid hydrogels using copper free click chemistry for cartilage tissue engineering. *Polymer Chemistry* **9**, 20–27 (2018).
36. Wang, N. X. & von Recum, H. A. Affinity-Based Drug Delivery. *Macromolecular Bioscience* **11**, 321–332 (2011).
37. Vulic, K. & Shoichet, M. S. Affinity-Based Drug Delivery Systems for Tissue Repair and Regeneration. *Biomacromolecules* **15**, 3867–3880 (2014).
38. Edelman, E. R., Mathiowitz, E., Langer, R. & Klagsbrun, M. Controlled and modulated release of basic fibroblast growth factor. *Biomaterials* **12**, 619–626 (1991).
39. Lin, C.-C. & Metters, A. T. Bifunctional Monolithic Affinity Hydrogels for Dual-Protein Delivery. *Biomacromolecules* **9**, 789–795 (2008).
40. Lin, C. & Metters, A. T. Metal-chelating affinity hydrogels for sustained protein release. *Journal of Biomedical Materials Research Part A* **83A**, 954–964 (2007).
41. Koehler, K. C., Anseth, K. S. & Bowman, C. N. Diels–Alder Mediated Controlled Release from a Poly(ethylene glycol) Based Hydrogel. *Biomacromolecules* **14**, 538–547 (2013).
42. Huynh, V. & Wylie, R. G. Competitive Affinity Release for Long-Term Delivery of Antibodies from Hydrogels. *Angew Chem Int Ed Engl* **57**, 3406–3410 (2018).
43. Huynh, V. & Wylie, R. G. Displacement Affinity Release of Antibodies from Injectable Hydrogels. *ACS Applied Materials & Interfaces* **11**, 30648–30660 (2019).
44. Huynh, V., Jesmer, A. H., Shoaib, M. M. & Wylie, R. G. Influence of Hydrophobic Cross-Linkers on Carboxybetaine Copolymer Stimuli Response and Hydrogel Biological Properties. *Langmuir* **35**, 1631–1641 (2019).
45. Jain, A., Barve, A., Zhao, Z., Jin, W. & Cheng, K. Comparison of Avidin, Neutravidin, and Streptavidin as Nanocarriers for Efficient siRNA Delivery. *Molecular Pharmaceutics* **14**, 1517–1527 (2017).
46. Zhang, Y. *et al.* Fundamentals and applications of zwitterionic antifouling polymers. *Journal of Physics D: Applied Physics* **52**, 403001 (2019).
47. Shao, Q. & Jiang, S. Influence of Charged Groups on the Properties of Zwitterionic Moieties: A Molecular Simulation Study. *The Journal of Physical Chemistry B* **118**, 7630–7637 (2014).
48. Zhang, L. *et al.* Zwitterionic hydrogels implanted in mice resist the foreign-body reaction. *Nature Biotechnology* **31**, 553–556 (2013).
49. Cao, B., Tang, Q. & Cheng, G. Recent advances of zwitterionic carboxybetaine materials and their derivatives. *Journal of Biomaterials Science, Polymer Edition* **25**, 1502–1513 (2014).
50. Ladd, J., Zhang, Z., Chen, S., Hower, J. C. & Jiang, S. Zwitterionic Polymers Exhibiting High Resistance to Nonspecific Protein Adsorption from Human Serum and Plasma. *Biomacromolecules* **9**, 1357–1361 (2008).
51. Vaisocherová, H. *et al.* Ultralow Fouling and Functionalizable Surface Chemistry Based on a Zwitterionic Polymer Enabling Sensitive and Specific Protein Detection in Undiluted Blood Plasma. *Analytical Chemistry* **80**, 7894–7901 (2008).

52. Zhang, Z., Chen, S. & Jiang, S. Dual-Functional Biomimetic Materials: Nonfouling Poly(carboxybetaine) with Active Functional Groups for Protein Immobilization. *Biomacromolecules* **7**, 3311–3315 (2006).
53. Yang, W., Xue, H., Carr, L. R., Wang, J. & Jiang, S. Zwitterionic poly(carboxybetaine) hydrogels for glucose biosensors in complex media. *Biosensors and Bioelectronics* **26**, 2454–2459 (2011).
54. Truong, N. P., Jones, G. R., Bradford, K. G. E., Konkolewicz, D. & Anastasaki, A. A comparison of RAFT and ATRP methods for controlled radical polymerization. *Nature Reviews Chemistry* **5**, 859–869 (2021).
55. Moad, C. L. & Moad, G. Fundamentals of reversible addition–fragmentation chain transfer (RAFT). *Chemistry Teacher International* **3**, 3–17 (2021).
56. Perrier, S. *50th Anniversary Perspective* : RAFT Polymerization—A User Guide. *Macromolecules* **50**, 7433–7447 (2017).
57. Perrier, S. *50th Anniversary Perspective* : RAFT Polymerization—A User Guide. *Macromolecules* **50**, 7433–7447 (2017).
58. Sun, Y., Nan, D., Jin, H. & Qu, X. Recent advances of injectable hydrogels for drug delivery and tissue engineering applications. *Polymer Testing* **81**, 106283 (2020).
59. Agard, N. J., Prescher, J. A. & Bertozzi, C. R. A Strain-Promoted [3 + 2] Azide−Alkyne Cycloaddition for Covalent Modification of Biomolecules in Living Systems. *J Am Chem Soc* **126**, 15046–15047 (2004).
60. Huynh, V., Jesmer, A. H., Shoaib, M. M. & Wylie, R. G. Influence of Hydrophobic Cross-Linkers on Carboxybetaine Copolymer Stimuli Response and Hydrogel Biological Properties. *Langmuir* **35**, 1631–1641 (2019).
61. Huisgen, R. 1,3-Dipolar Cycloadditions. Past and Future. *Angewandte Chemie International Edition in English* **2**, 565–598 (1963).
62. Hao, L. *et al.* Albumin-binding prodrugs via reversible iminoboronate forming nanoparticles for cancer drug delivery. *Journal of Controlled Release* **330**, 362–371 (2021).
63. Cal, P. M. S. D. *et al.* Iminoboronates: A new strategy for reversible protein modification. *J Am Chem Soc* **134**, 10299–10305 (2012).
64. Cambray, S. & Gao, J. Versatile Bioconjugation Chemistries of ortho-Boronyl Aryl Ketones and Aldehydes. *Accounts of Chemical Research* **51**, 2198–2206 (2018).
65. Bandyopadhyay, A. & Gao, J. Iminoboronate Formation Leads to Fast and Reversible Conjugation Chemistry of α-Nucleophiles at Neutral pH. *Chemistry* **21**, 14748–52 (2015).
66. Schmidt, P., Stress, C. & Gillingham, D. Boronic acids facilitate rapid oxime condensations at neutral pH. *Chemical Science* **6**, 3329–3333 (2015).
67. Shoaib, M. M. *et al.* Controlled degradation of low-fouling poly(oligo(ethylene glycol)methyl ether methacrylate) hydrogels. *RSC Advances* **9**, 18978–18988 (2019).
68. Almagro, J. C., Daniels-Wells, T. R., Perez-Tapia, S. M. & Penichet, M. L. Progress and Challenges in the Design and Clinical Development of Antibodies for Cancer Therapy. *Frontiers in Immunology* **8**, (2018).
69. Chen, Y. & Liu, L. Modern methods for delivery of drugs across the blood–brain barrier. *Advanced Drug Delivery Reviews* **64**, 640–665 (2012).
70. Begley, D. J. & Brightman, M. W. Structural and functional aspects of the blood-brain barrier. in *Peptide Transport and Delivery into the Central Nervous System* 39–78 (Birkhäuser Basel, 2003). doi:10.1007/978-3-0348-8049-7_2.

71. Lampson, L. A. Monoclonal antibodies in neuro-oncology. *MAbs* **3**, 153–160 (2011).
72. Pan, W. & Kastin, A. J. Changing the chemokine gradient: CINC1 crosses the blood–brain barrier. *Journal of Neuroimmunology* **115**, 64–70 (2001).
73. Puts, M. T. E. *et al.* Factors influencing adherence to cancer treatment in older adults with cancer: a systematic review. *Annals of Oncology* **25**, 564–577 (2014).
74. Blanford, J. I., Kumar, S., Luo, W. & MacEachren, A. M. It's a long, long walk: accessibility to hospitals, maternity and integrated health centers in Niger. *International Journal of Health Geographics* **11**, 24 (2012).
75. Public Health Ontario. Vaccine Storage and Handling Guidelines. *https://www.health.gov.on.ca/en/pro/programs/publichealth/oph_standards/docs/reference/vaccine%20_storage_handling_guidelines_en.pdf*.
76. Al-Taiar, A., Clark, A., Longenecker, J. C. & Whitty, C. J. Physical accessibility and utilization of health services in Yemen. *International Journal of Health Geographics* **9**, 38 (2010).
77. Peck, M. *et al.* Global Routine Vaccination Coverage, 2018. *MMWR. Morbidity and Mortality Weekly Report* **68**, 937–942 (2019).
78. Zhang, J. *et al.* A pulsatile release platform based on photo-induced imine-crosslinking hydrogel promotes scarless wound healing. *Nature Communications* **12**, 1670 (2021).
79. Cal, P. M. S. D., Frade, R. F. M., Cordeiro, C. & Gois, P. M. P. Reversible Lysine Modification on Proteins by Using Functionalized Boronic Acids. *Chemistry - A European Journal* **21**, 8182–8187 (2015).
80. Ranieri, G. *et al.* Vascular Endothelial Growth Factor (VEGF) as a Target of Bevacizumab in Cancer: From the Biology to the Clinic. *Current Medicinal Chemistry* **13**, 1845–1857 (2006).
81. Meng, F. & Lowell, C. A. Lipopolysaccharide (LPS)-induced Macrophage Activation and Signal Transduction in the Absence of Src-Family Kinases Hck, Fgr, and Lyn. *Journal of Experimental Medicine* **185**, 1661–1670 (1997).
82. Achilli, C., Ciana, A., Fagnoni, M., Balduini, C. & Minetti, G. Susceptibility to hydrolysis of phenylboronic pinacol esters at physiological pH. *Open Chemistry* **11**, 137–139 (2013).
83. Greg T. Hermanson. *Bioconjugate Techniques*. (Elsevier, 1996). doi:10.1016/B978-0-12-342335-1.X5000-3.
84. Vashist, S. K., Dixit, C. K., MacCraith, B. D. & O'Kennedy, R. Effect of antibody immobilization strategies on the analytical performance of a surface plasmon resonance-based immunoassay. *Analyst* **136**, 4431 (2011).
85. Wang, Y., Fei, D., Vanderlaan, M. & Song, A. Biological activity of bevacizumab, a humanized anti-VEGF antibody in vitro. *Angiogenesis* **7**, 335–345 (2004).
86. Finco, D. *et al.* Cytokine release assays: Current practices and future directions. *Cytokine* **66**, 143–155 (2014).
87. Grimaldi, C. *et al.* Cytokine release: A workshop proceedings on the state-of-the-science, current challenges and future directions. *Cytokine* **85**, 101–108 (2016).
88. del Amo, E. M. & Urtti, A. Rabbit as an animal model for intravitreal pharmacokinetics: Clinical predictability and quality of the published data. *Experimental Eye Research* **137**, 111–124 (2015).

5 Appendix

5.1 Supplementary Figures

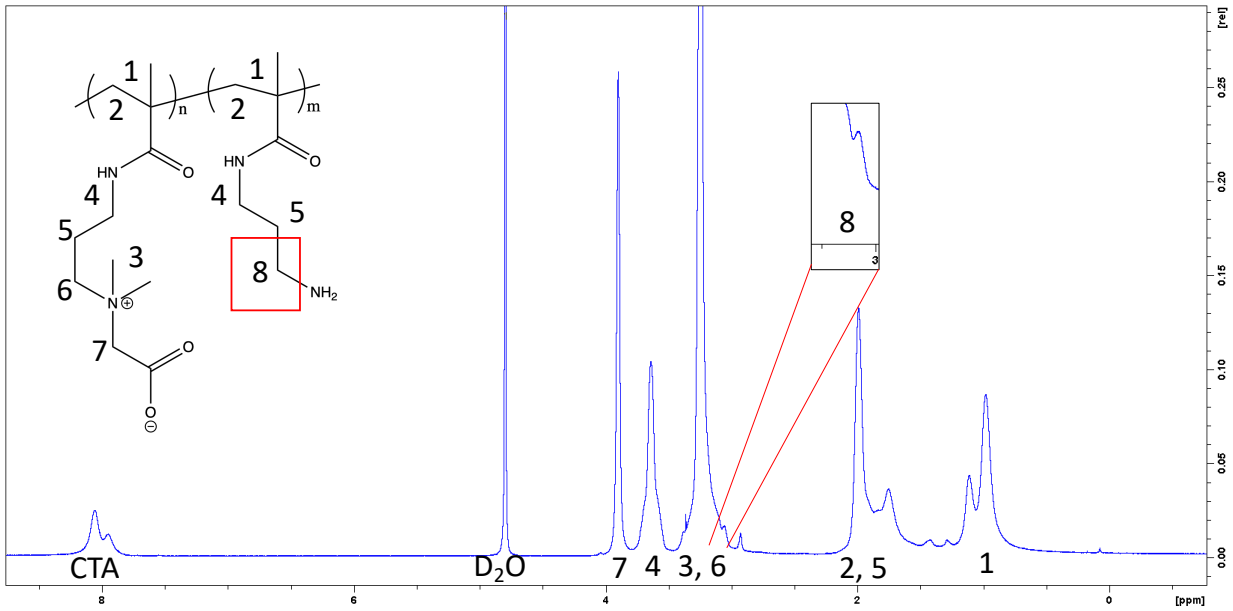

A. ^{1}H NMR spectrum of pCB-APMA

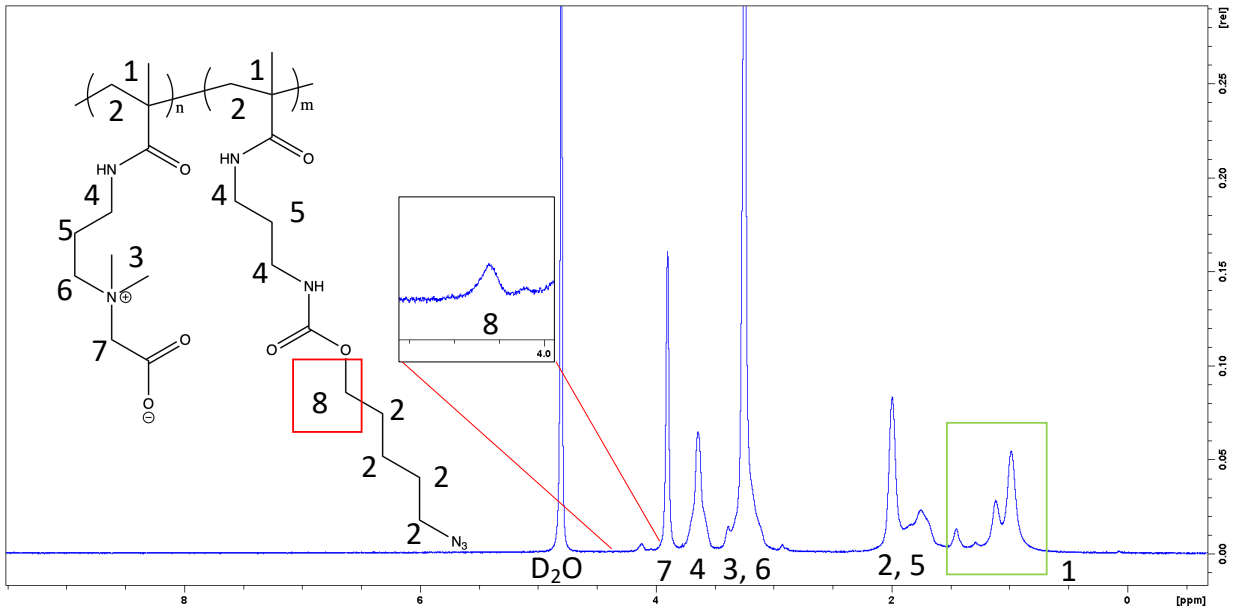

B. ^{1}H NMR spectrum of pCB-azide

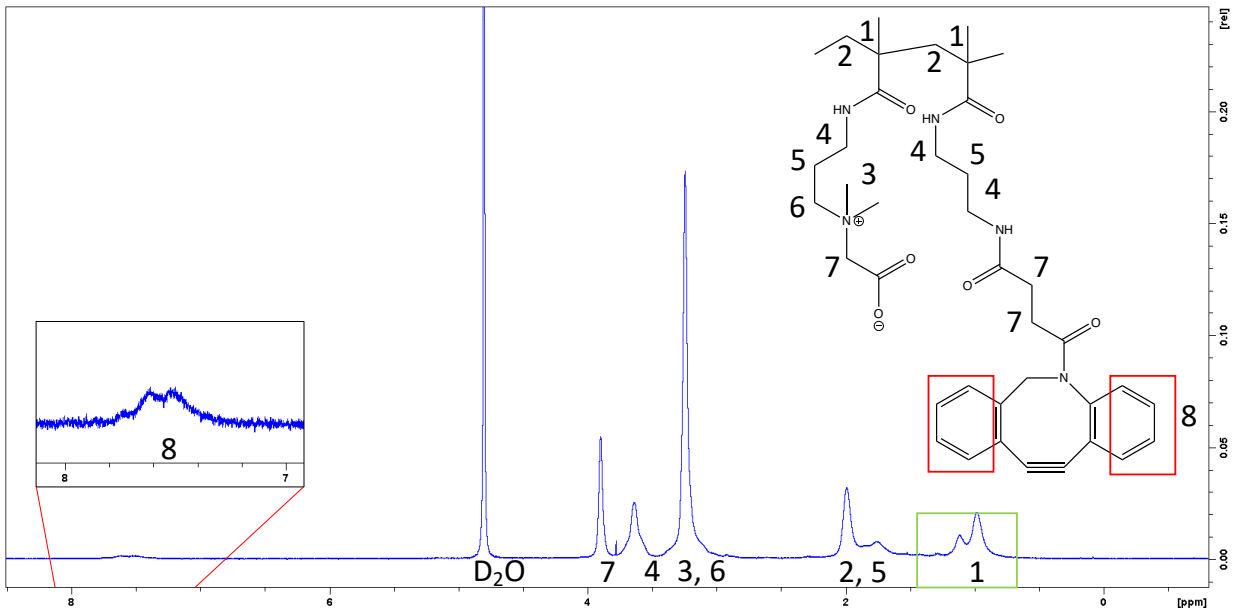

C. ^{1}H NMR spectrum of pCB-DBCO

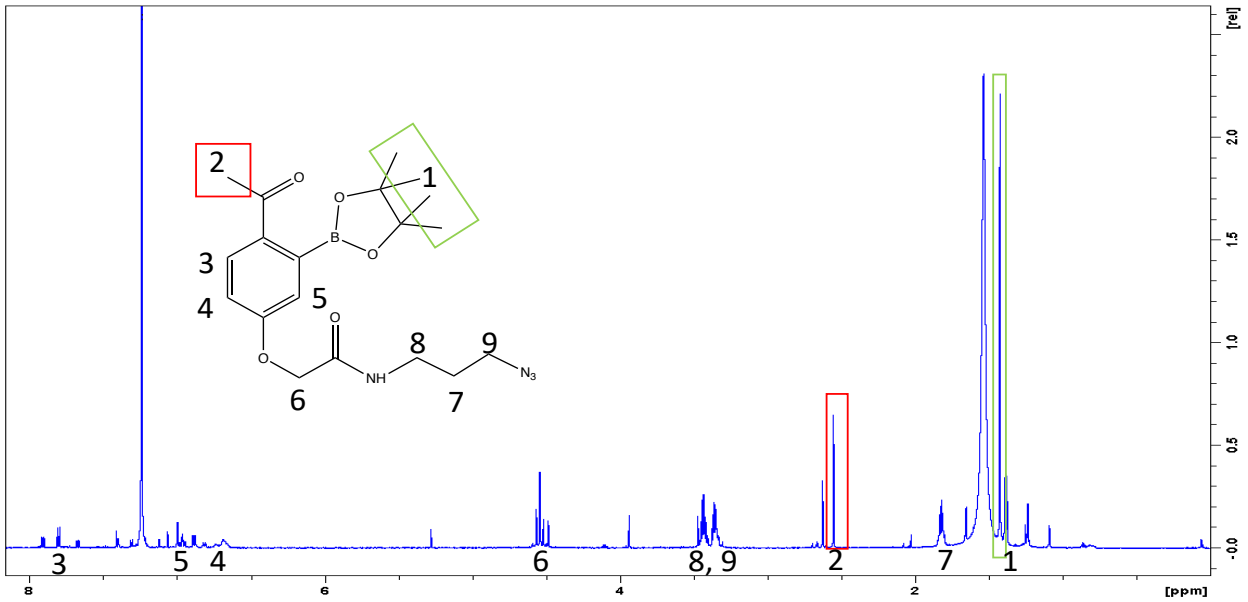

D. ^{1}H NMR spectrum of azido pinacol 2-APBA ester

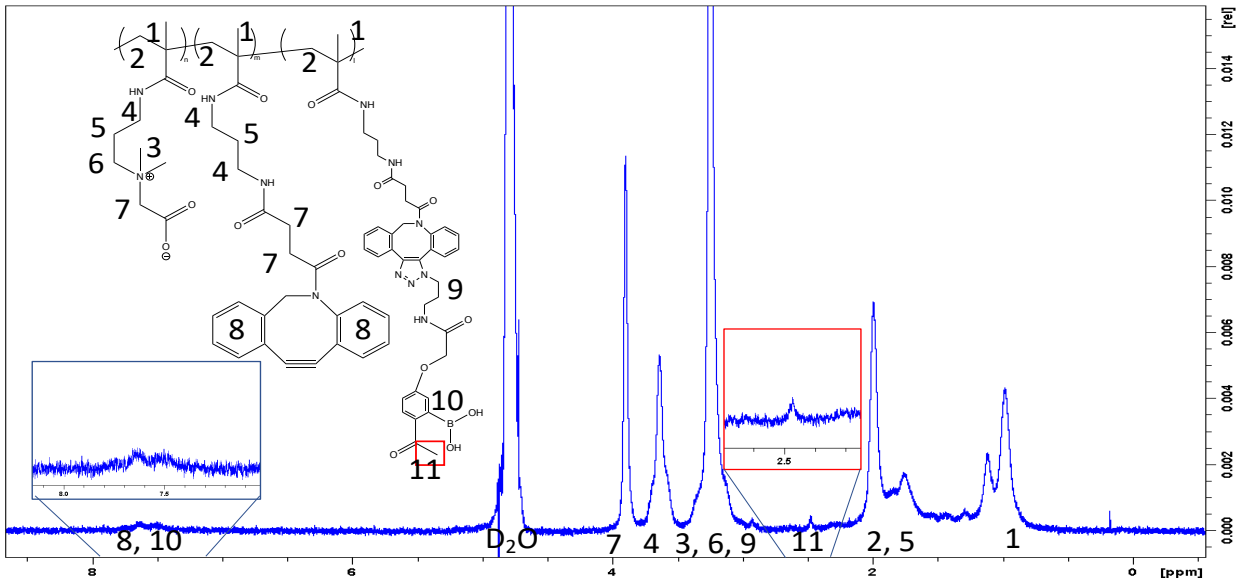

E. ^{1}H NMR spectrum of pCB-(2-APBA)-DBCO

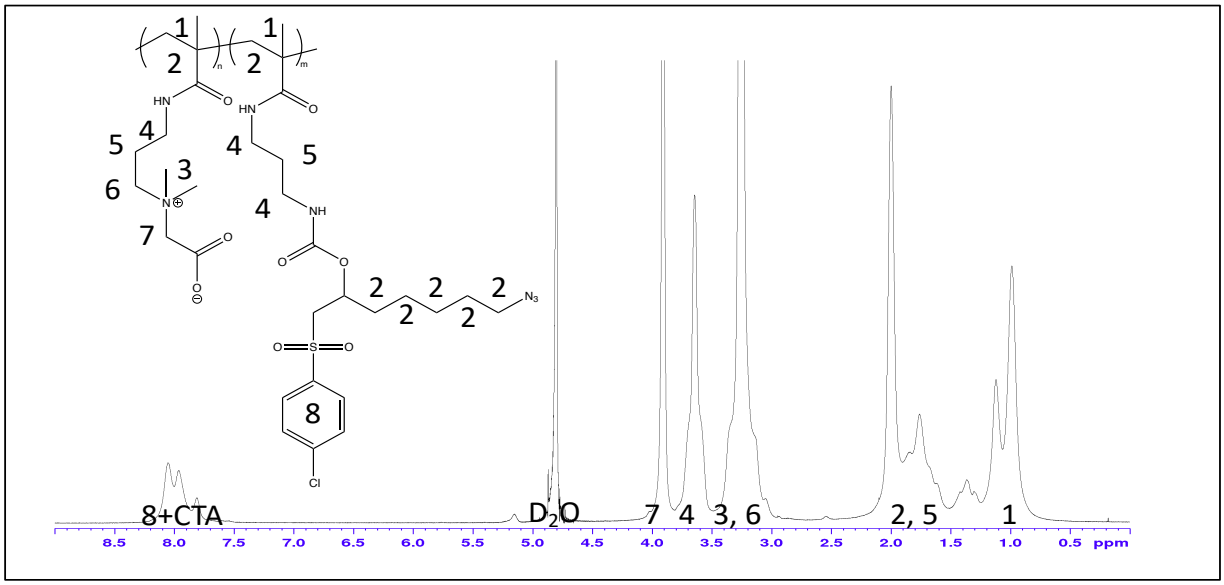

F. ^{1}H NMR spectrum of pCB-azide (Cl)

Figure S 1. ^{1}H NMR spectra of polymers and small molecule crosslinkers.

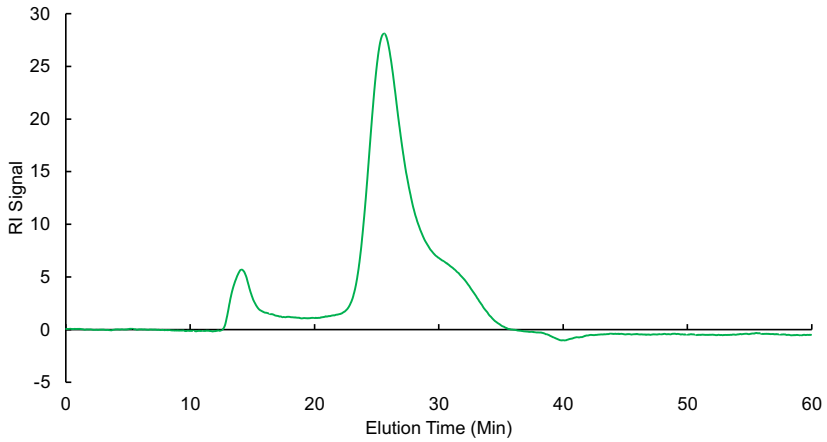

Figure S 2. Gel permeation chromatography (GPC) spectrum of pCB-APMA

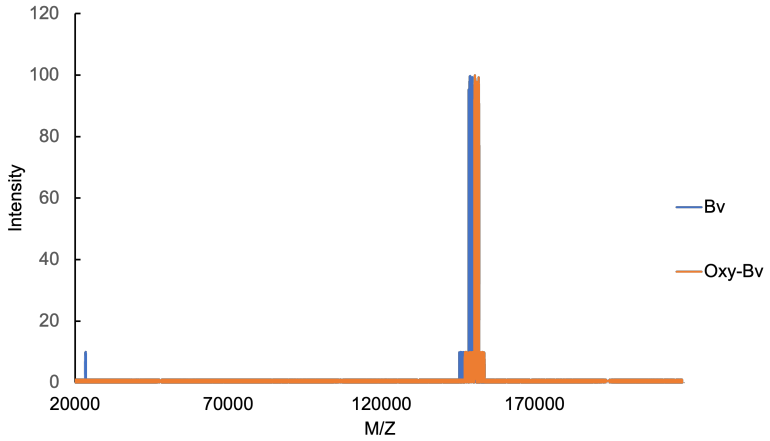

Figure S 3. MALDI spectrum of Oxy-Bv conjugates

Table S 1. Summary of average oxyamine conjugation number on bevacizumab (Bv). Molar mass of Bv and Oxy-Bv were detected via MALDI-MS.

Oxy-Bv m/z (kDa)	Bv m/z (kDa)	Mass Increase (kDa)	# conjugation
151.1	149.1	2.03	23

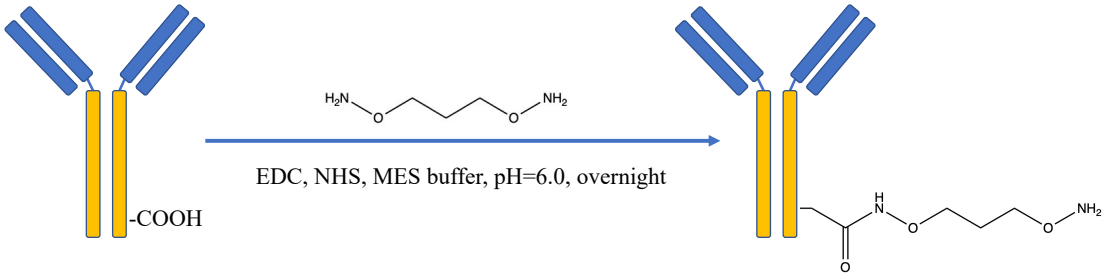

Figure S 4. Schematic of Oxy-Bv synthesis

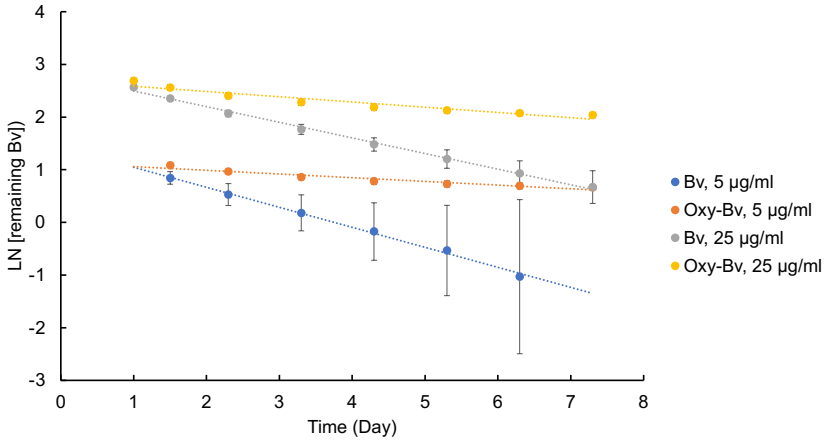

Figure S 5. Linear relationship between time and LN [remaining Bv] after burst release

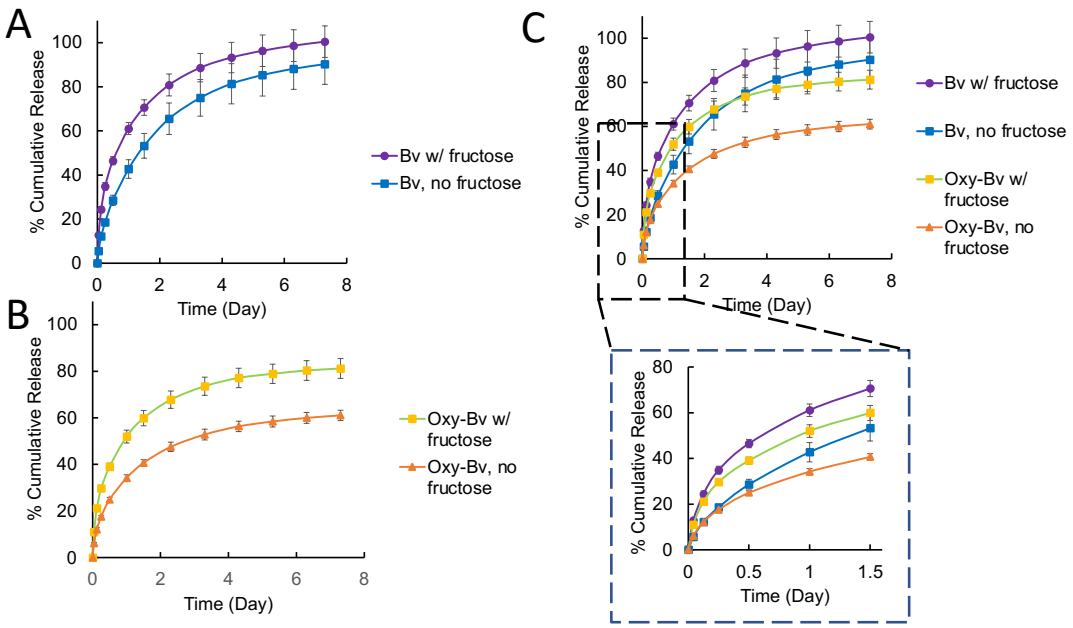

Figure S 6. Fructose-in-buffer displacement release. Presence of fructose in supernatant (5.3 mM) was shown to accelerate release rate of antibodies incapsulated within pCB-APBA hydrogel. 5 μg/ml of (A) Bv and (B) Oxy-Bv were reversibly immobilized onto pCB-APBA hydrogel with or without fructose in supernatant, and in both conditions, presence of fructose corresponds to greater release rate of Bv derivative. Addition of fructose allowed (C) greater burst release rate on Day 1 among both Bv and Oxy-Bv, although stronger bond between Oxy-Bv and APBA might lead to lower sustained release rate as evident in its slower depletion.

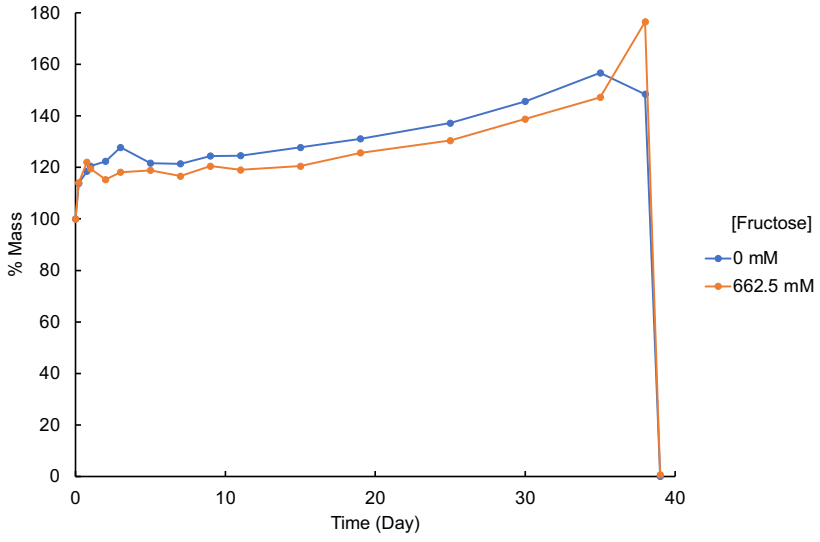

Figure S 7. Degradation time of pCB-APBA hydrogel from crosslinked pCB-Az (Cl) and pCB-APBA-DBCO